Isometric and Dynamic Contraction Muscle Fatigue Assessment Using Time-frequency Methods

by

Hiroko Austin

A Thesis Presented in Partial Fulfillment
of the Requirements for the Degree
Master of Science in Engineering

Approved November 2012 by the
Graduate Supervisory Committee:

Antonia Papandreou-Suppappola, Chair
Narayan Kovvali
Jitendran Muthuswamy

ARIZONA STATE UNIVERSITY

December 2012

ABSTRACT

The use of electromyography (EMG) signals to characterize muscle fatigue has been widely accepted. Initial work on characterizing muscle fatigue during isometric contractions demonstrated that its frequency decreases while its amplitude increases with the onset of fatigue. More recent work concentrated on developing techniques to characterize dynamic contractions for use in clinical and training applications. Studies demonstrated that as fatigue progresses, the EMG signal undergoes a shift in frequency, and different physiological mechanisms on the possible cause of the shift were considered. Time-frequency processing, using the Wigner distribution or spectrogram, is one of the techniques used to estimate the instantaneous mean frequency and instantaneous median frequency of the EMG signal using a variety of techniques. However, these time-frequency methods suffer either from cross-term interference when processing signals with multiple components or time-frequency resolution due to the use of windowing.

This study proposes the use of the matching pursuit decomposition (MPD) with a Gaussian dictionary to process EMG signals produced during both isometric and dynamic contractions. In particular, the MPD obtains unique time-frequency features that represent the EMG signal time-frequency dependence without suffering from cross-terms or loss in time-frequency resolution. As the MPD does not depend on an analysis window like the spectrogram, it is more robust in applying the time-frequency features to identify the spectral time-variation of the EGM signal.

To My children, Shota, Kurumi, Joe

and

My husband, Jon and My parents.

ACKNOWLEDGEMENTS

First, I would like to thank Dr. Antonia Papandrou-Suppappola for giving me the opportunity to do this work. Her guidance, support and encouragement were always there when I needed it. I would like to thank Dr. Narayan Kovvali for helping me to understand the material and MATLAB programming. Every day I had many questions. I would like to thank Dr. Jitendran Muthuswamy for his interest in my research and for agreeing to serve as a member of my committee. I would like to thank Dr. Veronica Santos for letting me use her laboratory and instruments and supporting my study. Graduate students in Dr. Papandrou-Suppappola's laboratory and Dr. Santos's laboratory, thank you for your support. I would like to thank my children, Shota, Kurumi, and Joe for supporting this work by doing all the tasks around the house for me and taking extra responsibilities. Finally, I would like to thank my husband, Jon, for support, encouragement, and guidance.

TABLE OF CONTENTS

LIST OF TABLES

LIST OF FIGURES

Chapter 1

INTRODUCTION

1.1 Overview and Motivation

Most people have experienced muscle fatigue at one time or another. People know when they have fatigue but it is not easy to measure and quantify. If a reliable and reproducible measurement process can be developed, it will have wide ranging applications. Monitoring the localized fatigue of muscles could be a very important tool for workers who perform repetitive physical tasks and for athletes who are training to improve their performance. Such a measurement can help to avoid injury due to muscle fatigue and over use. Also, in rehabilitation medicine, monitoring muscle fatigue is very important especially for patients with neuromuscular problems. The efficacy of exercise treatment depends on exercising the muscle that needs the therapy. In some cases, other muscles may compensate for the weak muscle during treatment, denying the targeted muscle the therapy required by proper exercising. Monitoring muscle fatigue using EMG technology is one way to evaluate the therapy being used.

Researchers have been investigating the assessment of localized muscle fatigue in humans using surface electromyography (sEMG) signals during constant force isometric contraction [1–3] and dynamic contraction [2]. As early as 1912, a physiologist used electromyography to observe the characteristics of muscle fatigue during constant force isometric contraction [1,2]. He observed a shift to lower frequencies in the spectral content of the sEMG signal. This phenomenon was subsequently observed in different body muscles by numerous researchers [1,2,4]. In the 1950s, it was observed that the amplitude of the electromyography signal increases over time for an isometric contraction [1, 2, 5]. The early research was done on isometric contractions to avoid problems associated with the signal complexity of dynamic contraction sEMG signals. Advances in computer technology have made it possible to use digital signal

processing methods to evaluate the spectral content of sEMG signals [2]. At first, this kind of analysis was used on data from constant force isometric contractions to assess fatigue [2]. During constant force isometric contraction, sEMG signals are non- stationary, in that they have frequency components that change with time. frequency component. However, the assumption of stationary for short time segments has been applied to enable analysis as it allows the use of Fourier transforms [1,2,4]. The fast Fourier transform (FFT) was one of the tools used for this research. Using FFT confirmed the shift in the sEMG spectral content to lower frequencies as measured by the mean frequency or the median frequency of the spectrum [6]. The sEMG signals for dynamic contractions have components that result from changes in the length of the muscle fibers, in the distance from the electrode to the muscle fiber, and in the force applied by the muscle that result from change in geometry as the exercise progresses [7]. As dynamic contractions involve non-stationary signals [2,8–10], they require analysis using more advanced signal processing techniques such as time-frequency (TF) methods. Examples with TF methods used successfully for sEMG analysis include the Winger distribution(WD), Choi-Williams distribution and wavelet transforms [2, 9, 10]. Even with the progress to date, researchers continue to try to improve the reliability, reproducibility and convenience of these analysis techniques to enable their standardization and use in clinical and training applications [4]. Further challenges in this field are centered on four areas.

1. Improved characterization of the way that the signal changes during exercise to improve detection of the onset of fatigue; most current techniques sample data at various epochs to provide a quasi-stationary window of data for analysis assuming that sEMG signals during isometric and dynamic contractions are non-stationary [4].

2. Reduction of the variability of techniques [4, 11].

3. Simplification and standardization of the methods used; for example, different

techniques were recommended in [12] depending on the contraction modality.

4. Extension of signal processing methods to encompass a wider variety of movements, and in particular increased angular velocity and increased force [9].

Time-frequency signal processing have been used to determine the fatigue progress using the sEMG spectrum. These time-frequency approaches have different disadvantages depending on the method. These disadvantages include cross terms and poor TF resolution [2, 8] that make interpretation of the results difficult. Investigators have tried a number of techniques for data collection and analysis to reduce these effects. The results are acceptable but limited to specific situations, often requiring special equipment to collect the data to minimize variability [12]. Monitoring the change of frequency of the signal over time was implemented using the mean frequency or median frequency as indicators [2]. With the use of TF methods, those measures were replaced by instantaneous mean frequency or instantaneous median frequency [12, 13]. The instantaneous mean frequency is the same as instantaneous frequency which is the average frequency at each time [13]. This method works well for monocomponent signals but problems were reported for multi component signals due to the existence of cross terms or because the TF methods did not satisfy important signal properties [13]. A method that overcomes these problems, without increasing complexity in data collection or analysis requirements would provide for better means to study sEGM signal characteristics.

1.2 Proposed Work

The objective of this study is to investigate the use of the matching pursuit decomposition (MPD) for analyzing sEMG signals during muscle isometric and dynamic contractions to assess localized muscle fatigue. The MPD technique has advantages over previously investigated techniques by offering improved resolution

in time and frequency, especially for non-stationary signals [14]. The corresponding MPD time-frequency representation (MPD-TFR) is implemented by summing the weighted WD distribution TF representation of each MPD expanded signal component. The MPD-TFR thus does not suffer from cross terms and offers high TF resolution since these components correspond to Gaussian signals and the WD of a Gaussian has the highest TF resolution [15]. We estimation the average frequency from the MPD-TFR was using the weighted average instantaneous frequency method to improve variability. This work compared the performance of MPD technique for fatigue detection with that of existing techniques such as the spectrogram.

1.3 Thesis Organization

The rest of the thesis is organized as follows. Chapter 2 discusses sEMG signals and muscle fatigue. Chapter 3 provides a background on current methods used for processing sEMG signals to assess muscle fatigue. The methods differ based on whether the signal originated from constant force isometric contractions or dynamic contractions. Chapter 4 describes the matching pursuit decomposition and its use for time-frequency signal processing. Chapter 5 provides our proposed use of the MPD to obtain time-frequency features for sEMG signal analysis. Chapter 6 discusses and compares the analysis performance results of our work using real data, and summary of the experimental procedures used to obtain the data is provided. It includes summary of experimental information and procedure. Chapter 7 presents conclusion and recommendation for future work.

Chapter 2

ELECTROMYOGRAPHY AND MUSCLE FATIGUE

2.1 Electromyography

Electromyography (EMG) is the measurement of the electrical activity in the muscle fibers induced by activation of the motor neurons innervating the muscle [1]. Bioelectric potential exhibits a resting potential and action potential when appropriately simulated. But EMG signals contain noise due to electrical currents traveling through different layer tissues [8]. Physiologically, an EMG signal is the summation of the signal motor unit action potential (MUAP) for the muscle fibers activated during a contraction. The MUAPs are the result of depolarization in muscle fibers. This occurs when alpha-motoneurons in the spinal cord transmit a signal to activate the muscle. Figure 2.1 shows a model of the generation of the EMG signal [1].

The alpha-motoneurons affect the output of the EMG signal shape by controlling the unit firing rate with impulse timing and the number of the motor units affected. The muscle can only continue to contract if the motor units are activated repeatedly to sustain the effort. The series of MUAP events is called a motor unit action potential train (MUAPT). The number of muscle fibers that are activated and the timing of those activations affect the EMG signal [1]. In skeletal muscles, the composition of the muscle and the blood flow are also factors that affect the EMG signals. The muscle fibers are divided into two functional groups, slow twitch and fast twitch or type I and type II, respectively. Type I muscle fibers are slow twitch fibers with long contraction duration and are resistant to fatigue. The nerve conduction velocity is lower for slow twitch muscle fibers [4]. On the other hand, the type II muscle fibers, which are divided to type IIa and type IIb, are fast twitch with short contraction duration. Type IIa fibers have good fatigue resistance but type IIb, which are used for power and speed, fatigue easily [4, 16]. The nerve conduction velocity for type IIa and type IIb fibers is intermediate and high, respectively [4].

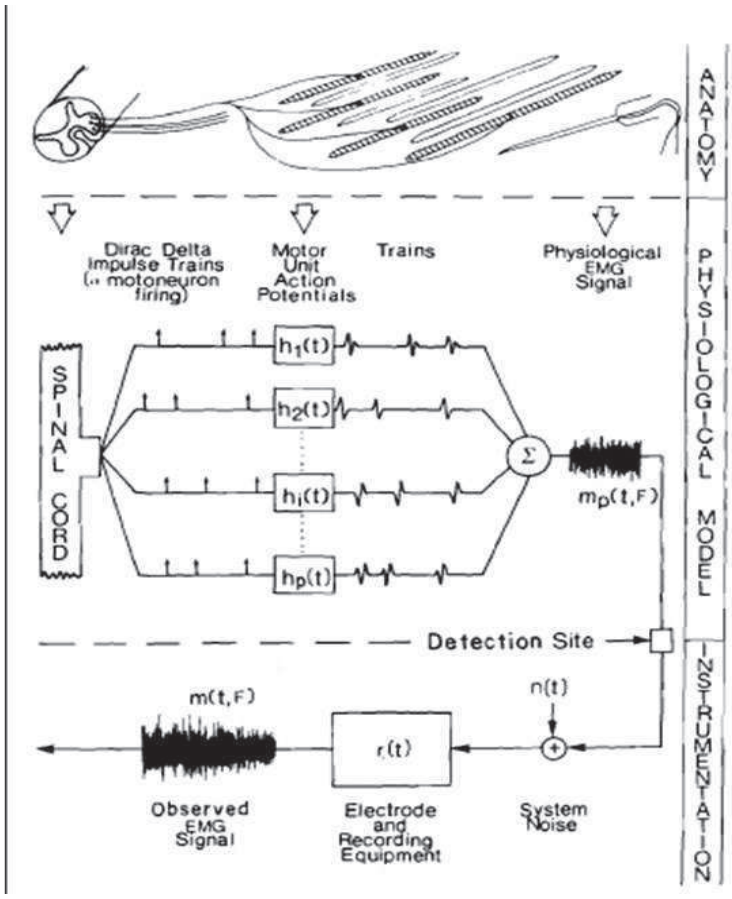

Figure 2.1: The model for the generation of the EMG signal obtained from [1]

The components of these muscle types depend on the individual and are related to exercise activities and aging. Researchers observed a relationship between use of muscle types and level of muscle contractions [4]. It was shown that slow twitch muscle fibers are depleted of glycogen at 15% to 20% of maximum voluntary contraction [4]. The spectrum of the sEMG signal is probably affected by both the type of exercise and the muscle types recruited for the movement. Other physiological and biochemical factors also affect sEMG signals. The structure of muscle fibers is different in different muscle parts and in different individuals. The mechanism of how these differences affect the EMG signal is not yet completely understood and is the subject of ongoing scientific investigations [2]. Another important factor in the collection and analysis of sEMG signals is the position of electrodes and electrode

shape as well as the distance between muscle fiber and electrode which is related to the thickness of the subcutaneous tissue [1, 8]. All of these factors contribute to the complications associated with the analysis of sEMG signals.

The unit of measurement of the sEMG signal is voltage and its range is from 0 to 10 mV (+5 to -5) [8]. The sEMG signal is not only the result of the physiological phenomena of muscle movement. It also contains noise from power line circuits and electronic equipment, noise induced on the connecting cables as well as noise from other sources. Electronic equipment generate noise that is very difficult to reduce or eliminate. High quality equipment suffer from less noise but they are expensive. The noise caused by electromagnetic radiation that could be present can affect the sEMG signal because the amplitude can be higher than the magnitude of the original signal by a factor of three to one [8]. The average alpha-motoneuron firing rate is 15 to 25 Hz [17], and it creates the 20 Hz signal component [8,17] which can cause the signal to be unstable in this region. The motion artifact from the electrode interface and movement of the electrode cable affects the low frequency region of the signal [8]. To avoid noise in the low frequency part of the signal, filtering with low-frequency cut-off of 20 Hz is recommended [8, 17]. It is possible to eliminate some noise from the signal but not all using filtering and skin preparation where the electrodes are attached [18].

The position of the electrodes can also contribute to noise. One electrode is placed on the mid line of the muscle between the myotendenous junction and the point of innervation, perpendicular to the fibers of the muscle [17]. The electrode for the ground is placed on the skin over the bone. Modern EMG instrumentation amplifies and filters the signal.

2.2 Muscle Fatigue

Fatigue occurs when a task is repeated over and over again. People can feel fatigue, but it is very difficult to measure the magnitude of fatigue or pinpoint its onset. Fatigue has been identified in a variety of ways. Some investigators use the inability of the muscle to sustain the task as a measure of fatigue. Other definitions use degradation of performance as an indicator of fatigue. However, the onset of fatigue in muscles is gradual [1]. Performance changes gradually as the relaxed muscle gradually becomes less effective and then cannot sustain contraction. This feeling is well known to athletes in training. Thus, any scientific measure of fatigue needs to monitor change in some muscle characteristic over time. The traditional mechanism proposed for the cause of fatigue is the accumulation of lactic acid in the muscle tissue. Lactic acid is a byproduct of the metabolism of sugars to provide energy for muscle movement. Lactic acid is further decomposed to water and carbon dioxide when it reacts with oxygen. This is the situation during aerobic exercise. The result of localized muscle fatigue shows that the power spectrum of the sEMG signal is shifted to lower frequencies. Researchers have been investigating what kind of physiological component is affecting the power spectrum of sEMG signals. Researchers found a positive correlation between the low frequency shift in the power spectrum of the sEMG signal and the decreases in muscle fiber conduction velocity (MFCV) during static sustain construction [19]. As lactate builds up in the muscle cells, the pH or measure of hydrogen ions decreases causing the conduction velocity of the de-polarization reaction to decrease. This changes the profile of the MUAP, which affects the sEMG signal recorded from the muscle. The effects of decreased pH on conduction velocity as well as the EMG frequency shift to lower frequencies in [20]. Numerous studies have been done to asses localized muscle fatigue and relate it to sEMG signal and physiological factors, especially the effects of conduction velocity and firing rate [2]. Other investigators believe that the decrease in pH is

only a factor when maximal exertion is applied [16]. For dynamic contraction, it was shown that no change was seen in MFCV whereas median frequency (MDF) of the power spectrum of the sEMG signal decreased from the vastus lateralis of 19 health male adults [19]. These alternate theories propose that fatigue is a complex phenomenon with contributing factors in both the central and peripheral nervous systems [16]. These factors include psychological factors, neural signal transmission factors and failure of transmission of the signal from the nerve to the muscle [16]. In any case, sEMG measurements are useful for measuring the behavior of the muscle fibers. If reliable measurement and processing techniques are developed to measure and characterize fatigue, they can contribute to understanding the mechanisms of fatigue.

Chapter 3

TIME-FREQUENCY PROCESSING OF SEMG SIGNALS

3.1 Instantaneous Mean and Median Frequency

A century ago, a physiology professor named Piper at the Royal Friedrich-Wilhelms University in Berlin found that the spectral content of sEMG signals shifts towards low frequencies over time during constant isometric contraction [1, 2]. Increased signal amplitude during constant force isometric contraction as a characteristic of fatigue as well as compression of frequency toward the lower range was observed [1, 2]. These two phenomena related to muscle fatigue manifestation are the most popular methods of fatigue detection. In [21], the frequency of mean power or mean frequency (MNF) was used to determine the difference between a relaxed muscle and a fatigued muscle during constant isometric contraction. Fatigued muscles were characterized by having power spectrum in the lower half of the frequency range, whereas relaxed muscles were observed to have power spectrum in the upper half of the spectrum [21]. The MNF for fatigue was lower than the MNF of relaxed muscle [21]. The median frequency (MDF), the MNF, and the mode (peak) frequency of the spectrum were investigated by theoretical analysis in [22], where it was shown that the MDF was the preferred frequency estimate because it was least sensitive to noise compared to the rest of the estimates [21]. The MDF and MNF are the most widely used parameters, and they can be defined respectively as the average frequency and a frequency point that divides power spectrum into two equal parts.

During last decade, the instantaneous mean frequency (IMNF) and instantaneous median frequency (IMDF) time-frequency signal processing methods were introduced for determining localized fatigue during dynamic contraction [2]. The MNF, MDF, IMNF, and IMDF are defined in [2] as,

$$\mathrm{MNF}_{s(t)} = \frac{\int_0^{f_s/2} f S(f) \mathrm{d}f}{\int_0^{f_s/2} S(f) \mathrm{d}f} \tag{3.1}$$

$$\int_0^{\mathrm{MDF}_{s(t)}} S(f)\mathrm{d}f = \int_{\mathrm{MDF}_{s(f)}}^{\infty} S(f)\mathrm{d}f \tag{3.2}$$

$$\mathrm{IMNF}_{(t)} = \frac{\int_0^{\infty} fS(t,f)\mathrm{d}f}{\int_0^{\infty} S(t,f)\mathrm{d}f} \tag{3.3}$$

$$\int_0^{\mathrm{IMDF}_{(t)}} S(t,f)\mathrm{d}f = \int_{\mathrm{IMDF}_{(t)}}^{\infty} S(t,f)\mathrm{d}f, \tag{3.4}$$

where f_s is the sampling frequency, $S(f)$ is power spectrum density of the signals, and $S(t,f)$ is time-dependent power spectrum density of the signal.

The methods used for estimating the power spectral density (PSD) of sEMG signals for detection of local fatigue include the periodogram and Blackman-Tukey method [23]. Parametric model PSD estimation methods include the autoregressive (AR), moving average (MA), and autoregressive moving average (ARMA) methods [23]. The sEMG signal during constant force isometric contraction is not stationary since frequency changes with respect to time [2, 7, 9, 24]. However, sEMG characteristics during constant force isometric contraction can be considered as Gaussian wide-sense stationary (WSS) and band-limited with zero mean over a short segment of time [2, 12] or epoch [24, 25]. During constant force isometric contraction, the stationary segments were shown to range from 0.5 to 2 seconds depending on the contraction force level and muscle characteristics [9]. It was also observed that the length changes with different levels of contractions [3]. A length of 20-40 seconds can be WWS at 20%-30% MVC while 0.5-1.5 seconds is at 50%-80% MVC [3]. To allow the use of any PSD estimation process, a signal needs to be time-invariant and stationary [1, 23]. Applying PSD estimation methods to a sEMG signal, which is non-stationary, can be done using windowing of the signal assuming stationarity within the windowed segment Accuracy and reliability of the result depends on the shape and size of the analysis window, and it affects the estimation of MNF and MDF [26,27]. The periodogram is the most commonly used method; it is the squared magnitude of Fourier transform of windowed segments.

ARMA is combination of the AR and MA models and it is quite powerful [2, 24]. The selection of the order of the model affects variance and accuracy. The estimated spectrum appears overly smooth when the order is too small. On the other hand, the variance increases and artificial peaks appear [2,24]. The AR model is often chosen for sEMG processing with order between 4 and 11 [2,24].

In the time domain, the amplitude of the sEMG signal was observed during constant force isometric contraction [1, 2, 18, 24]. The sEMG amplitude metrics in modern digital systems are the mean absolute value (MAV) and root-mean-squared (RMS) value. One of the main problems in the amplitude analysis method is rejecting noise suppression; noise sources can include power line interference, electronic noise and motion artifacts. A cascade of five sequential processing steps were developed to form a sEMG amplitude estimate [2,18]. The steps are noise rejection and filtering, whitening, amplitude demodulation, smoothing and linearization. The whitening process reduces the variance of the amplitude estimation [18, 25, 28]. In most cases, both amplitude and spectrum analysis are used together [2]. To make sEMG analysis useful in clinical settings, joint analysis of sEMG spectrum and amplitude (JASA) for isometric exercises was divided to four different cases to simplify analysis. It was found that if the sEMG spectrum shifts to the higher frequency and sEMG amplitude increases, the reason is due to the increased force. If the sEMG spectrum shifts to a lower frequency and the sEMG amplitude decreases, the most probable cause is a decrease in muscle force. When the sEMG spectrum shifts to a lower frequency and the sEMG amplitude increases, then the cause is fatigue. Finally, when the sEMG spectrum shifts to a higher frequency and the sEMG amplitude decreases, this is an indication of recovery from fatigue. These simple rules are used to relate changes in the spectrum and amplitude to actual muscle conditions during isometric exercise [2]. This result was extended to extend this result to dynamic repetitive tasks [29]. However, there simple rules could not be used for classification.

In [29], the frequency shift by MNF and MDF could not be detected using the wavelet transform method and a decrease in amplitude for all subject was noted due to the absence of constant force [29]. Overall, the estimation results obtained the sEMG spectrum content are less dependent on the force level of muscle compared to the estimation results obtained from the sEMG amplitude and are more sensitive for detection of muscle fatigue [30, 31].

3.2 Short time Fourier Transform

The short time Fourier transform (STFT) is a linear time-frequency representation(TFR) that was used to study fatigue during isometric and isotonic muscle contractions. The studies showed that the frequency content of the sEMG signal decreased with increased fatigue [32]. The STFT assumes that the sEMG signal is stationary over a short windowed signal segment and then analyzes each segment with the Fourier transform [9]. TFRs represent signals in both time and frequency. Thus, the STFT with analysis window $h(t)$ is given by

$$S_x(t, f; h) = \int_\tau e^{-j2f\pi\tau} x(\tau) h(\tau - t)\, \mathrm{d}\tau, \tag{3.5}$$

The STFT preserves time-frequency shifts on the signal [33],

$$y(t) = x(t - t_o)e^{j2\pi f_o t} => S_y(t, f; h) = S_x(t - t_o, f - f_o; h)e^{-j2\pi t_o(f-f_o)}. \tag{3.6}$$

However, the STFT does not preserve energy information and it is limited by assumption of signal stationarity over the length of the window [2, 33–35]. Following the uncertainty inequality, given as

$$\Delta T \Delta\omega \geq \frac{1}{2} \tag{3.7}$$

where $\omega = 2\pi f$, if the window is chosen to have a narrow bandwidth to increase frequency resolution, then the time resolution decreases since the window has long duration [30, 33]. This trade off presents a problem in fatigue analysis since the desirable use is to detect changes in the frequency content; if the changes are small, the high

frequency resolution is needed but at the cost of low time resolution. Wavelet based methods were also used to study frequency changes for fatigue analysis [30]. The STFT and continuous wavelet transform (CWT) were used to analyze mechanomyographic (MMG) and sEMG signals collected from the vastus lateralis and rectus femoris muscles during isometric ramp contractions [36]. A Hamming window of 0.6s was used by the STFT, with an overlap of 0.1 s, and the resulting TFR was used to estimate the mean power frequency (MPF) at each time. The instantaneous mean power frequency was calculated using the CWT and compared to the MPF estimate of the STFT. Frequency shifting to lower frequencies was not observed in this experiment. As TFRs, both the CWT and the STFT showed similar results, although the STFT provided better representation using fixed resolution [36]. However, the wavelet is only useful for multiresolution analysis, desiring different frequency resolutions at different times, and this was not shown to be needed for fatigue analysis. Note, also, that the wavelet transform also uses windowing and thus still has time-frequency resolution trade off.

3.3 Quadratic TFRs

The spectrogram is a quadratic TFR that is obtained as the squared magnitude of the STFT

$$\mathrm{SP}_{s(t,f;h)} = |S_x(t,f;h)|^2. \tag{3.8}$$

It belongs to a class of TFRs, called Cohen's class, that preserve time-frequency shifts on the analysis signal [35]. These TFRs are characterized by a unique kernel $\phi_C(\theta,\tau)$ and defined as

$$\mathrm{C}(t,f) = \int_{-\infty}^{\infty}\int_{-\infty}^{\infty}\int_{-\infty}^{\infty} e^{-j2\pi(\theta\upsilon+\tau f-\theta t)}\phi_C(\theta,\tau)x^*(\upsilon-\frac{1}{2}\tau)x(\upsilon+\frac{1}{2}\tau)\mathrm{d}\upsilon\mathrm{d}\tau\mathrm{d}\theta \tag{3.9}$$

Based on the kernel function, a TFR can be chosen to satisfy different desirable signal properties such as preservation of signal energy. The kernel for the spectrogram is

in terms of its window $h(t)$, and it is given by

$$\phi_{\mathrm{SP}}(\theta,\tau)=\int h^{*}(\upsilon-\frac{1}{2}\tau)h(\upsilon+\frac{1}{2}\tau)e^{-j2\pi\theta\upsilon}\mathrm{d}\upsilon. \tag{3.10}$$

Equation (3.8) can be obtained by inserting (3.10) in (3.9) [34]. The time and frequency marginal properties relate to energy preservation and are thus important to satisfy if signal information needs to be recovered. The time-marginal and frequency marginal can be satisfied when $\phi(\theta,0)=1$ and $\phi(0,\tau)=1$, respectively. The spectrogram does not, in general, satisfy the marginal properties as it requires a constraint on its window $h(t)$. For example, for the spectrogram to satisfy the time marginal, the window must satisfy the condition $\int|h(t)|^{2}e^{j2\pi\theta t}dt=1$, for all θ. For the spectrogram to preserve the signal's instantaneous frequency, both $\phi(0,\tau)=1$ and $\frac{\partial}{\partial\tau}\phi(\tau,\upsilon)|_{\tau}=0$ must be satisfied; it is thus difficult to find a window size and shape that satisfies these requirements.

Several comparisons between the STFT and other TFR methods during isometric and dynamic contraction have been done. The Wigner distribution (WD), Choi-Williams distribution (CWD) and the STFT distribution were all applied to the sEMG signals collected from biceps brachii during an isometric contraction and were compared in [34]. It was found that all three approaches showed the frequencies decreases as time increases due to fatigue [34]. The CWD showed the shifting of the frequency toward to lower frequencies most effectively because the spread of frequency was less [34]. Note that all three TFRs produced different representations in the time-frequency plane [34].

The characterization of isometric contractions using sEMG signals has progressed from relatively primitive methods to sophisticated use of various TFR methods. The study of muscle fatigue during dynamic contractions only started in the last decade because the sEMG signals from dynamic contraction are very complex due to changes in the muscle length, force and distance between electrode and muscle during movement [3, 7]. For the non-stationary sEMG signals during dynamic con-

traction, Cohen's class TFRs and the wavelet transform provided useful results [2,3]. TFRs that were used to analyze EMG signals during dynamic contraction include the smoothed-pseudo WD(SPWD), the CWD, and the Born-Jordan TFR [7, 12], as well as the continuous wavelet transform [37].

The WD can be obtained when $\phi_{\mathrm{WD}}(\theta, \tau) = 1$; it can be defined as

$$WD_x(t, f) = \int_{-\infty}^{\infty} x\left(t - \frac{\tau}{2}\right) x\left(t + \frac{\tau}{2}\right) e^{-j2\pi f\tau}\, \mathrm{d}\tau \tag{3.11}$$

where $x(t)$ is the signal. The WD satisfies the marginal properties, preserves frequency shifts and time shifts is real-valued and it is highly localized in the time-frequency plane [33, 38]. However, the WD suffers from interfering cross terms when used the analyze multicomponent signals, which is the case for sEMG signals [7, 12, 33, 38]. This is a disadvantage of this method for analysis since a cross-interference term does not have any meaning and makes interpretation difficult. Cohen's class TFR formulation in refeq:spec2 provides a method to smooth the cross terms by using the kernel as a two-dimensional lowpass filter. One example is the SPWD that uses a time smoothing to obtain [38]

$$\mathrm{SPWVD}_x(t, f) = \iint w\left(t - \tau\right) g\left(f - \xi\right) W_x(\tau, \xi) \mathrm{d}\tau\, \mathrm{d}\xi. \tag{3.12}$$

The smoothing windows control time and frequency resolution separately. The resolution in time degrades as the smoothing in time increases. The same degradation occurs for frequency as the frequency window is increased [38]. The smoothing kernel for the CWD is

$$\phi_{\mathrm{CWD}}(\theta, \tau) = e^{(2\pi\theta\tau)^2}/\sigma \tag{3.13}$$

where σ is a parameter that can be selected for different levels of smoothing. The value of $\sigma = 1$ was used sEMG signal analysis in [7]. The CWD satisfies both the marginals and the instantaneous frequency and group delay properties [35]. Varying the σ parameter regulates the trade off between the suppression of interference terms

and time-frequency resolution. As σ increases, resolution increases but interference increases as well. At high values of σ, CWD approaches the WD [9].

In [7], robustness to noise of TFRs was investigated, including Born-Jordan TFR (BJ), CWD and WD. The kernel for the BJ TFR is

$$\phi(\theta, \tau) = \sin(\pi\theta\tau)/(\pi\theta\tau). \tag{3.14}$$

The BJ TFR minimizes the variance contributed by white noise [7]. The work used all three TFRs to calculate the root MSE from IMNF and the IMDF for four different known signals with added noise. The result showed the IMDF using the CWD is most preferable among those methods [7]. The goal of this study was to get reproducible results from TFRs for assessing localized muscle fatigue during dynamic contraction. The sEMG data was classified into slow non-stationary and fast non-stationary. The hypothesis was that the slow non-stationary was due to fatigue in the muscle. The fast non-stationary was attributed to biomechanical factors including muscle length, distance of the electrode from the muscle and changes of force on the muscle so it was proposed to eliminate the fast non-stationary portion of the signal. To avoid the fast non-stationary, the integration of the high frequency portion of the TFR was omitted using D'Alessio algorithm to estimate the upper frequency of the power spectrum [7]. In addition, the contractions were classified to highly fatiguing contractions and slowly fatiguing contractions. Highly fatiguing contractions are defined as maximal effort contractions where only a few cycles of the task can be performed. Slow fatiguing contractions are defined as contractions that can be performed for an extended number of cycles. For slowly fatiguing contractions, the estimation of IMNF and IMDF was computed using the data from a fixed portion of the exercise cycle. To further reduce variability, the result was averaged over a few consecutive cycles. The CWD was applied to real sEMG signals of the first dorsal interosseous muscle with these two methods described above. The result showed decreasing IMDF as the number of the repetitions increased. The estimation

of IMDF was affected by selecting different portions of each cycle. The standard deviation of the IMDF was reduced by half when averaging four IMDF consecutive repetitions [7]. The disadvantage of this approach is that it adds special equipment and requires a custom process for each type of activity evaluated.

When the CWT was used for dynamic contraction signals, it provided better analysis results than those of the WD and CWD [37]. In [38], the CWT, STFT and SPWVD, were used to detect muscle fatigue combined with independent component analysis (ICA), and artificial neural networks for isometric contraction. The result of detection was measured by accuracy, specificity, and sensitivity and all representations yielded similar results, revealing the possibility of detection of muscle fatigue [38].

Hilbert-Hung transform (HHT) was used to compute the MNF during isometric contractions [26] and dynamic contractions [39] and the result were compared with those obtained using Fourier and wavelet methods. The HHT was used to avoid the dependency of the other methods on selectable parameters; advantage of HHT is that quasi-stationary and linearity assumptions are not required [26,39]. Comparison showed low variability in HHT results. However, the empirical mode decomposition (EMD), which is a basic procedure of the HHT, was called into question on theoretical grounds [39].

One difficulty in analyzing sEMG signals is to identify and separate the noise from the physiological portion of the signal, especially during dynamic contraction. Sensitivity to noise can limit the robustness of the methods, but it is not realistic to completely distinguish noise from the real signal in the sEMG measurements. Another problem that many investigators encountered was the need to constantly adjust the analysis method to get acceptable results. A more consistent method can yield significant clinical advantages.

Chapter 4

TIME-FREQUENCY PROCESSING USING MATCHING PURSUIT DECOMPOSITION

4.1 Matching Pursuit Decomposition Algorithm

The matching pursuit decomposition (MPD) is an iterative algorithm that can be used to decompose a signal into a weighted linear expansion of element functions, selected from a complete and redundant dictionary [15]. The dictionary elements are most often time-frequency shifted and scaled versions of a basic Gaussian atom, and the linear expansion is formed using successive approximations of the signal with orthogonal projections on dictionary elements. The resulting expansion provides for highly-localized time-frequency features. This is because the decomposed elements are Gaussian signals that are known known to be the most concentrated signals in both time and frequency according to the uncertainty principle [35]. An example of a basic Gaussian atom in the time domain is shown in Figure 4.1. The MDP algorithm procedure is described next in more detail. We consider a time-varying finite-energy signal $x(t)$ that, can be represented using the MPD as

$$x(t) = \sum_{i=0}^{\infty} \alpha_i g_i(t). \tag{4.1}$$

Here, $g_i(t)$ is the Gaussian atom that is selected at the ith MPD iteration and α_i is the corresponding expansion coefficient. The MPD dictionary consists of the elements

$$g_{\boldsymbol{\theta}}(t) = g_{n,k,l}(t) = g\left(\zeta_l(t-\tau_n)\right) e^{-j2\pi\nu_k t}, \tag{4.2}$$

where $\tau_n \in \mathbb{R}$, $\nu_k \in \mathbb{R}$, and $\zeta_l \in \mathbb{R}$ are the nth time shift, kth frequency shift and lth scale change, respectively, on the basic Gaussian atom $g(t) = Ce^{-t^2}$ and $\boldsymbol{\theta} = [n\ k\ l]$ is a vector describing all three transformation parameters. The basic Gaussian atom $g(t)$ is centered at the origin of the time-frequency plane and is normalized to have unit energy using the constant C. Note that when using the MPD to process real

data, such as sEMG signals, then real Gaussian atoms are used to form the dictionary of the form,

$$g_{n,k,l}(t) = Ce^{-(\zeta_l(t-\tau_n))^2}\cos(2\pi\nu_k t). \tag{4.3}$$

The iterative procedure of the MPD first projects the analysis signal $x(t) = r_0(t)$ onto each element of the dictionary and selects $g_{\boldsymbol{\theta_0}}(t) = g_0(t)$ according to $g_{\boldsymbol{\theta_0}}(t) = \arg\max_{\boldsymbol{\theta}} |\langle r_0, g_{\boldsymbol{\theta}}\rangle|$, where $\langle r_0, g_{\boldsymbol{\theta}}\rangle = \int_{-\infty}^{\infty} r_0(t)g_{\boldsymbol{\theta}}(t)\mathrm{d}t$. This first extracted element, $g_0(t)$, is the Gaussian signal component with the highest energy signal contribution. The residual signal after the Gaussian atom extraction is $r_1(t) = x(t) - \alpha_0 g_0(t)$, where $\alpha_0 = \langle x, g_0\rangle$. The residual $r_1(t)$ is then decomposed in a similar manner as the signal $x(t)$. Similarly, at the ith iteration, $i = 0, 1, \ldots$, we decompose the ith residual signal $r_i(t) = \alpha_i g_i(t)$, where $g_i(t) = g_{\boldsymbol{\theta_i}}(t) = \arg\max_{\boldsymbol{\theta}} |\langle r_i, g_{\boldsymbol{\theta}}\rangle|$ and $\alpha_i = \langle r_i, g_i\rangle$.

The MPD signal after N iterations is given by

$$x(t) = \sum_{i=0}^{N-1} \alpha_i g_i(t) + r_N(t). \tag{4.4}$$

The energy E_x of the signal with normalized unit energy basis functions $g_i(t)$ after N MPD iterations is given by

$$E_x = (\|x\|_2)^2 = \sum_{i=0}^{N-1} |\alpha_i|^2 + (\|r_N\|_2)^2 \tag{4.5}$$

where $\|x\|_2 = \langle x, x\rangle$. Although for a complete representation, an infinite number of iterations is required [15], stopping criteria can be used to obtain a close signal representation. For example, the iterative process can be stopped when a large percentage of the signal's energy has already been extracted. This threshold provides an advantage to the MPD since it can be used to increase the signal-to-noise ratio (SNR) based on the noise level present in the data and the stopping criteria of the iterative algorithm [14, 15]. A quadratic time-frequency representation (TFR) can be obtained by forming the linear combination of the Wigner distribution (WD) of

each of the selected Gaussian atoms in the MPD expansion. The WD is defined as

$$\mathrm{WD}_x(t,f) = \int_{-\infty}^{\infty} .x\left(t-\frac{\tau}{2}\right) x\left(t+\frac{\tau}{2}\right) e^{-j2\pi f\tau}\,\mathrm{d}\tau. \tag{4.6}$$

It provides highly localized representations in the time-frequency plane, it does not depend on windowing, and it preserves time-frequency shifts and scale changes

$$y(t) = x(t-\tau) \rightarrow WD_y(t,f) = WD_x(t-\tau,f), \tag{4.7a}$$

$$y(t) = x(t)e^{j2\pi\nu t} \rightarrow WD_y(t,f) = WD_x(t,f-\nu), \tag{4.7b}$$

$$y(t) = \sqrt{|\zeta|}x(\zeta t) \rightarrow WD_y(t,f) = WD_x(t\zeta, f/\zeta). \tag{4.7c}$$

The WD of the Gaussian atoms can be found in closed-form by computing it analytically [15]

$$\mathrm{WD}_{g_{\boldsymbol{\theta}}}(t,f) = Ce^{-2\pi\zeta_l^2(t-\tau_n)^2}e^{-2\pi(f-\nu_k)^2/\zeta_l^2}. \tag{4.8}$$

An example of an MPD signal expansion and its MPD-TFR with iteration $N = 5$ for the original signal, $y(t) = 0.3\exp(-t^2 9.39^2)\cos(2\pi 52.5t) - 0.7\exp(-(t-0.3)^2 45.45^2)\cos(2\pi 152.5(t-0.3)) + 0.5\exp(-(t+0.25)^2 100^2).\cos(2\pi 302.5(t+0.25))$ are shown in Figure 4.2(g) and 4.2(h), respectively.

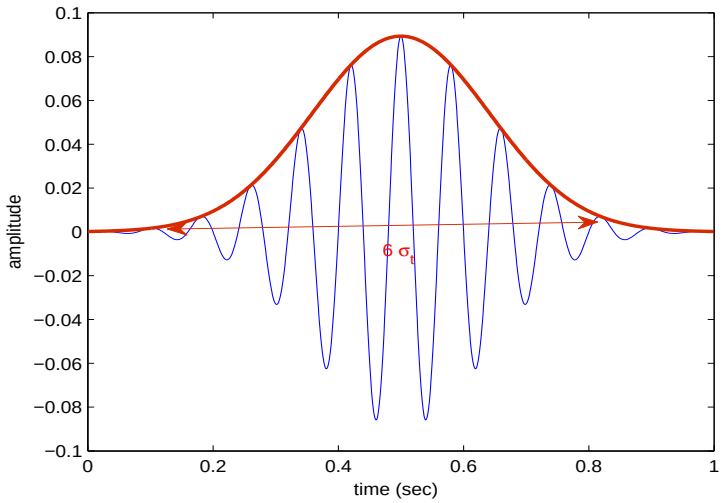

Figure 4.1: Example of a Gaussian atom in the MPD dictionary. The Gaussian atom is $g(t) = \frac{1}{11}e^{25t^2}\cos(6\pi t)$. The σ is one of the parameters for selecting Gaussian atoms.

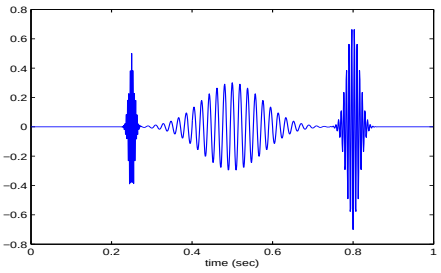

(a) original signal

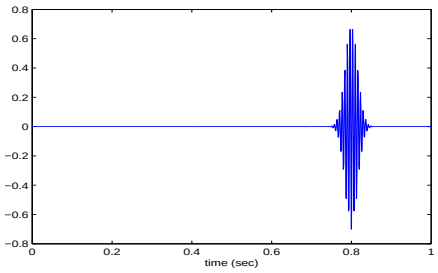

(b) $g_1(t)$

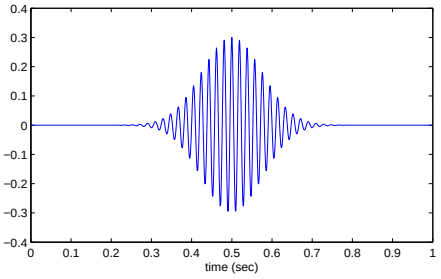

(c) $g_2(t)$

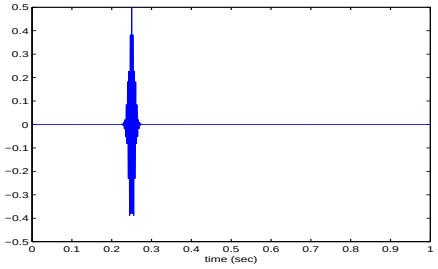

(d) $g_3(t)$

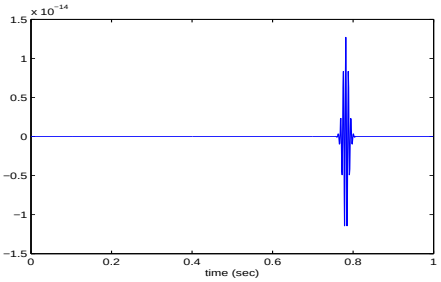

(e) $g_4(t)$

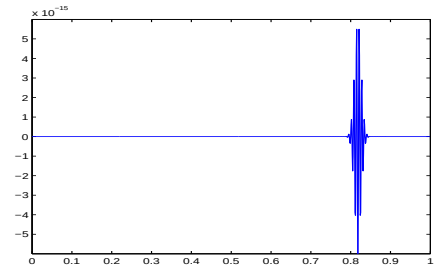

(f) $g_5(t)$

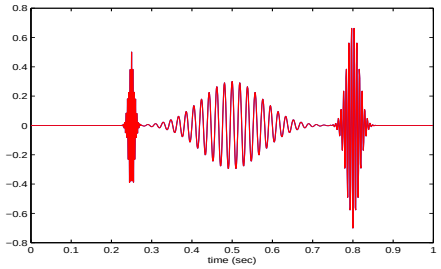

(g) MPD output after 5 iterations

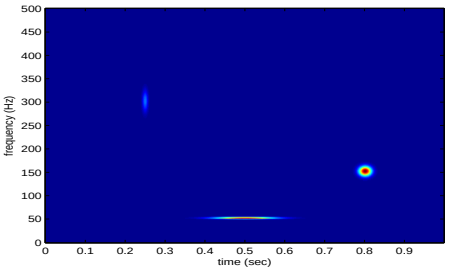

(h) MPD-TFR

Figure 4.2: Example of MPD: (a) original signal, (b)-(f) are the extracted Gaussian atoms, (g) original signal (blue line) and MPD approximation (red line) of signal after 5 iterations, (h) MPD-TFR

4.2 Instantaneous Frequency Using the MPD

Instantaneous frequency (IF) method is common for monitoring the frequency changes of the signal over time for non-stationary signals. The IF provides as average frequency at each time [40]. The traditional definition of IF for the analytic signal, $s(t) = a(t)e^{j\varphi(t)}$ is given by

$$f_i(t) = \frac{1}{2\pi}\frac{\mathrm{d}\varphi(t)}{\mathrm{d}t} = \varphi'(t). \tag{4.9}$$

The first central moment of a quadratic time-frequency representation (TFR) is IF and it can be defined by

$$F_i(t) = \frac{\int_{-\infty}^{\infty} fP(t,f)\mathrm{d}f}{\int_{-\infty}^{\infty} P(t,f)\mathrm{d}f}. \tag{4.10}$$

Note that the IF for quadratic TFRs is the exactly same as the IMNF Equation (3.3). Interpreting the IF as the average frequency at a given time for multicomponent signals is difficult [13, 40]. This traditional method uses the derivative of phase (4.9) to arrive at the average frequency for a given time. This method has the unfortunate attribute of occasionally giving a result for the average frequency that is outside of the range of the spectrum under certain circumstances for multicomponent systems [13, 40]. Clearly a method that gives a more reasonable result is desirable. Another problem with instantaneous frequency is that frequency oscillations per unit time imply that there is some non zero time over which the measurement is observed; instantaneous implies that delta t approaches zero [13]. A multicomponent signal can be expressed at the sum of two or more monocomponent signals and it can be written with assumption of each signal as analytic signal,

$$s(t) = \sum_{i=1}^{2} s_i(t), \tag{4.11}$$

where $s_i(t) = a_i(t)e^{j2\pi\varphi_i(t)}$.

The WD of a multicomponent signal which consists two monocomponent signals can be expressed as

$$W_{s_1+s_2}(t,f) = W_{s_1}(t,f) + W_{s_2}(t,f) + W_{s_1s_2}(t,f) + W_{s_2s_1}(t,f), \tag{4.12}$$

where $W_{s_1s_2}(t,f)$ and $W_{s_2s_1}(t,f)$ are the cross term that occurs from the multicomponent signal. The IF of the two component signals (4.10), obtained using the first order moment of TFRs is given by

$$F_i(t) = \frac{a_1^2(t)f_{i_1} + a_2^2(t)f_{i_2} + q(t)(f_{i_1}(t) + f_{i_2}(t))}{a_1^2(t) + a_2^2(t) + 2q(t)}, \tag{4.13}$$

where $q(t) = a_1(t)a_2(t)\cos(\varphi_1(t) + \varphi_2(t))$. The result of the IF for the multicomponent signal shows as an oscillating function and is sensitive to amplitude of the components of the signal [41] due to amplitude modulation. This highly non-linear IF for the multicomponent signal in Equation (4.13) does not provide a good interpretation of average frequency. The weighted average instantaneous frequency (WAIF) which can provide average frequency was given in [41]. The WAIF is defined as

$$f_w(t) = \frac{\sum_{i=0}^{N-1} a_i^2(t)\varphi_i'(t)}{2\pi\sum_{i=0}^{N-1} a_i^2(t)} \tag{4.14}$$

The WAIF is a summation of the individual first moment of the WD. It assumes that at each time point, there is only one frequency and it does provide true frequency content.

The first conditional spectral moment of the MPD-TFR result is WAIF [42]. The MPD of N iteration can be expressed as

$$x(t) = \sum_{i=0}^{N-1} \alpha_i g_i(t) = \sum_{h=0}^{2N-1} a_h(t)e^{j2\pi\varphi_h}(t), \tag{4.15}$$

where

$$a_h(t) = \alpha_h \frac{C}{2} e^{-\zeta_h^2 (t-\tau_h)^2}, h = 0, ...N-1, \tag{4.16a}$$

$$a_h(t) = \alpha_{h-N} \frac{C}{2} e^{-\zeta_{h-N}^2 (t-\tau_{h-N})^2}, h = N, ...2N-1, \tag{4.16b}$$

$$\varphi_h(t) = 2\pi\nu_h(t)t, h = 0, ...N-1, \tag{4.16c}$$

$$\varphi_h(t) = -2\pi\nu_{h-N}(t)t, h = N, ...2N-1. \tag{4.16d}$$

$$\tag{4.16e}$$

$a_h^2(t_1) \approx \alpha_h^2$ when $\tau_i = t_1$. The WAIF at $t = t_1$ from the MPD-TFR with a real Gaussian atom (4.3) can be expressed as

$$f_w(t_1) = \frac{\sum_{i=0}^{N-1} a_i^2(t_1)\varphi_i'(t_1)}{2\pi \sum_{i=0}^{N-1} a_i^2(t_1)} \approx \frac{\sum_{i=0}^{N-1} \alpha_i^2(t)\nu_i}{\sum_{i=0}^{N-1} \alpha_i^2(t)}. \tag{4.17}$$

The WAIF from the MPD gives a smoother result than the IF for multicomponent signals [42]. MPD expansion provides all relevant TF features that can be used to extract signal information.

Chapter 5

USE OF MPD FOR SEMG PROCESSING

In this thesis, we apply an advanced time-frequency based signal processing technique to increase our understanding of sEMG signals, both during isometric and dynamic contractions. It is important to improve the processing performance and increase the robustness of such techniques since understanding sEMG signals is critical in many clinical applications. These applications include studying muscular synergies in motor control during various tasks, estimating the extent of muscle damage under different stress or fatigue activities, and extracting features for use in the control of limb prosthesis [43].

5.1 MPD-based Approach

We propose to use the matching pursuit decomposition (MPD), presented in Chapter 4, as a technique to process the sEMG signals. Our approach is based on first applying the MPD with a Gaussian dictionary on a given sEMG signal to provide a linear weighted approximation of the signal. The expansion is in terms of time-frequency shift and scaled Gaussian atoms containing most of the signal's energy. In particular, the weight corresponding to each of these Gaussian atoms provides information on how strong the signal is at the time-frequency location where the Gaussian atom is centered.

5.1.1 Instantaneous Frequency From Features

Using the complete MPD signal expansion [15], the resulting vector of the time shift, frequency shift and scale change parameters for each extracted Gaussian atom provides unique time-frequency feature vectors for the expanded sEMG signal. In our work, we use these features to obtain a weighted average estimate of the signal's instantaneous frequency. The WAIF in Equation (4.14) which was presented

in Chapter 4 was used for this study. However, the WAIF $f_m(t)$ was modified to find an average frequency over a larger time interval. The modified WAIF for the interval was computed by using one frequency point which has the largest coefficient at each time and its coefficient. For example, for 9 iterations of MPD in an interval, 0 to 5 seconds, only five time and frequency shift parameters and coefficient are used as shown in Figure (5.1). The modified WAIF for this interval which is centered at 2.5 seconds is computed as $f_m(t)$ for $t = 2.5$ to obtain

$$f_m(2.5) = \frac{\alpha_1 f_1 + \alpha_5 f_5 + \alpha_9 f_9 + \alpha_6 f_6 + \alpha_3 f_3 + \alpha_7 f_7}{\alpha_1 + \alpha_5 + \alpha_9 + \alpha_6 + \alpha_3 + \alpha_7}, \tag{5.1}$$

using largest MPD coefficient and its frequency at each time in the interval (5.1).

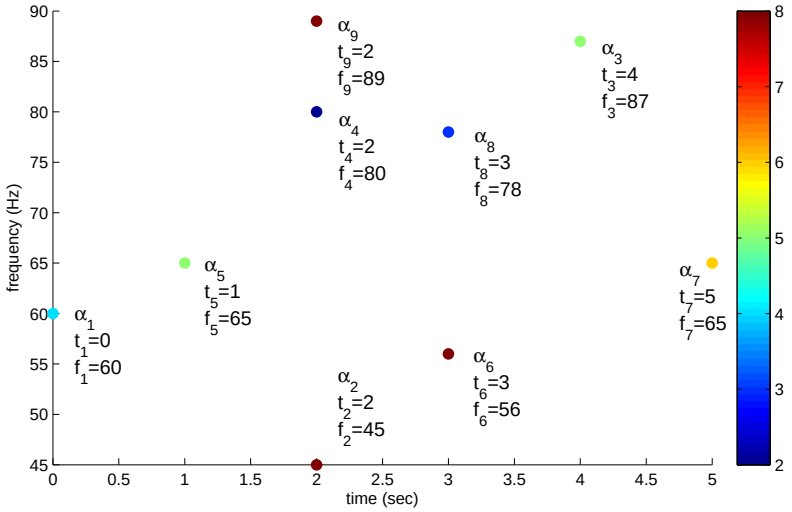

Figure 5.1: Example of modified WAIF

We used the modified WAIF for each interval to show the trend of frequency for isometric contractions. For dynamic contractions, one frequency point, which has the largest coefficient at a given time, was selected for that time. Then, the average frequency for one cycle of exercise was computed using the WAIF. The average frequency for each cycle was compiled to see the trend of frequency shift. A threshold in the coefficient value was applied to avoid the signal noise. Time and frequency

parameters for larger coefficients have more information about the signal compared to the time and frequency parameters for smaller coefficient. It is more likely that time and frequency parameters with smaller coefficients value correspond to noise. However, we do not want include noise in the WAIF computation, and as a result, several different threshold values were applied to extract the average frequency.

5.2 Isometric contraction data analysis

The original data shows 60 Hz noise and DC offset. First, the sEMG signals collected for all subjects were pre-processed removing the power line 60 Hz noise using a notch filter. The filter was designed as a second-order infinite impulse response (IIR) notch digital filter. The original sEMG signals and their Fourier transform (FT) for all subjects are shown in Figure 5.2 and Figure 5.3. After that, the data was filtered with a highpass filter to give the range from 10 Hz to 500 Hz. This process was done by using a 9th order Butterworth filter. The begin and end of the data string were processed to remove data where the subject was not exercising. Figure 5.6 shows the original signal, signal after filtering, signal after filtering and processing to remove data during periods of no exercise and the original signal and processed signal together for subject 2. The FT of the original signal, the signal after filtering and processing, and both signals plotted together for subject 2 are shown in Figure 5.7. The signal after filtering and its FT for all subjects are shown in Figure 5.4 and Figure 5.5 respectively.

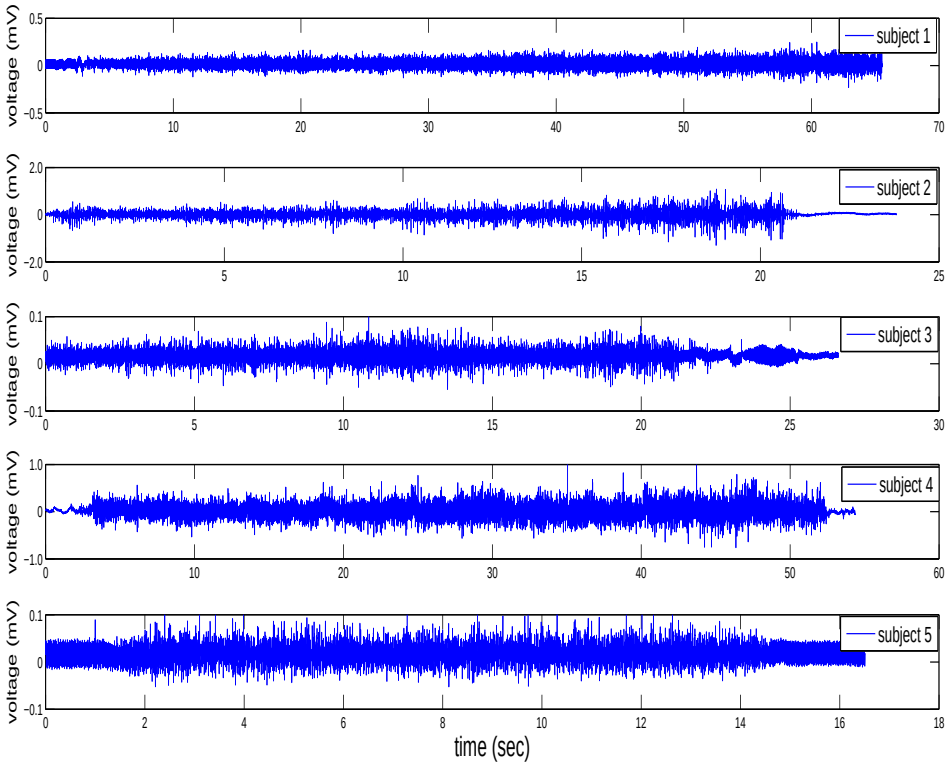

Figure 5.2: Isometric contraction original signal for all subjects

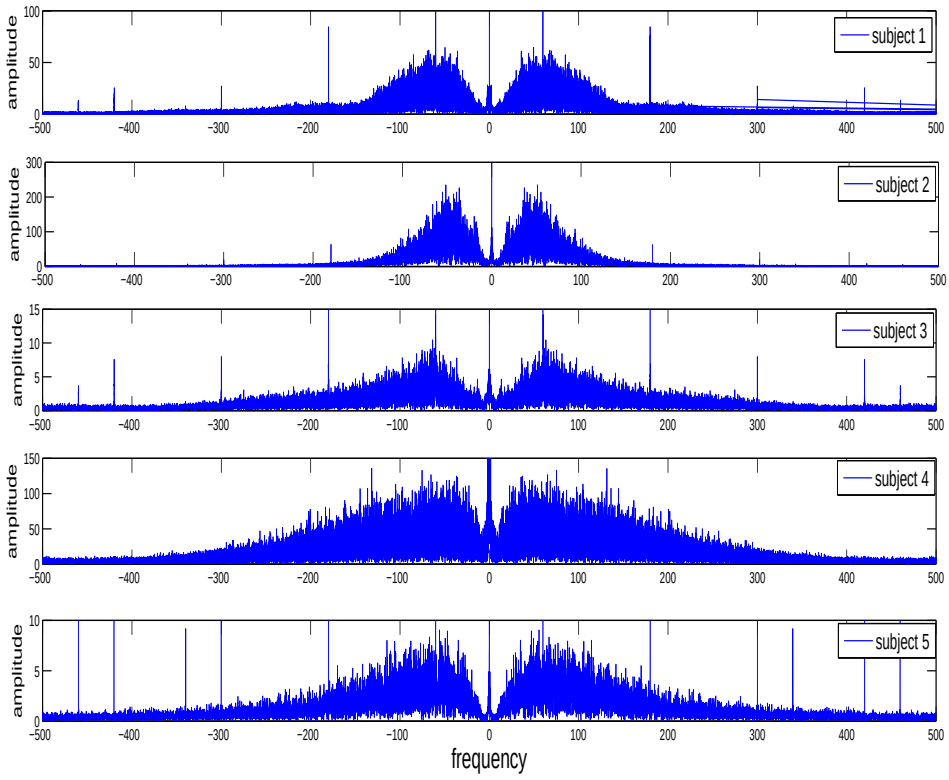

Figure 5.3: Isometric contraction original signal of FT for all subjects

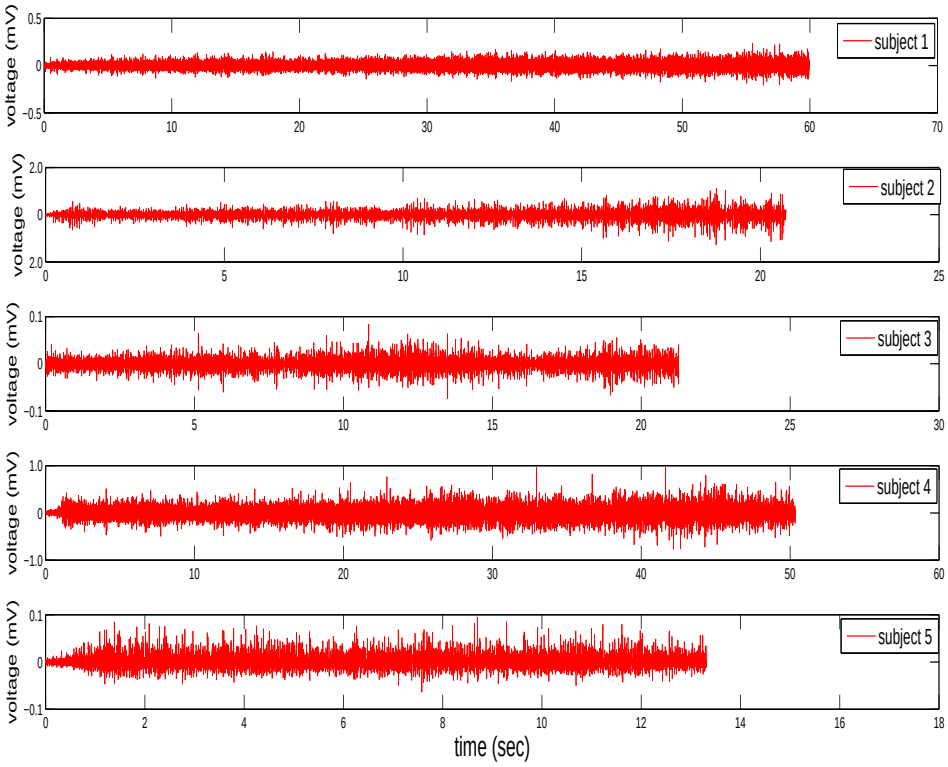

Figure 5.4: Isometric contraction after preprocessed for all subject

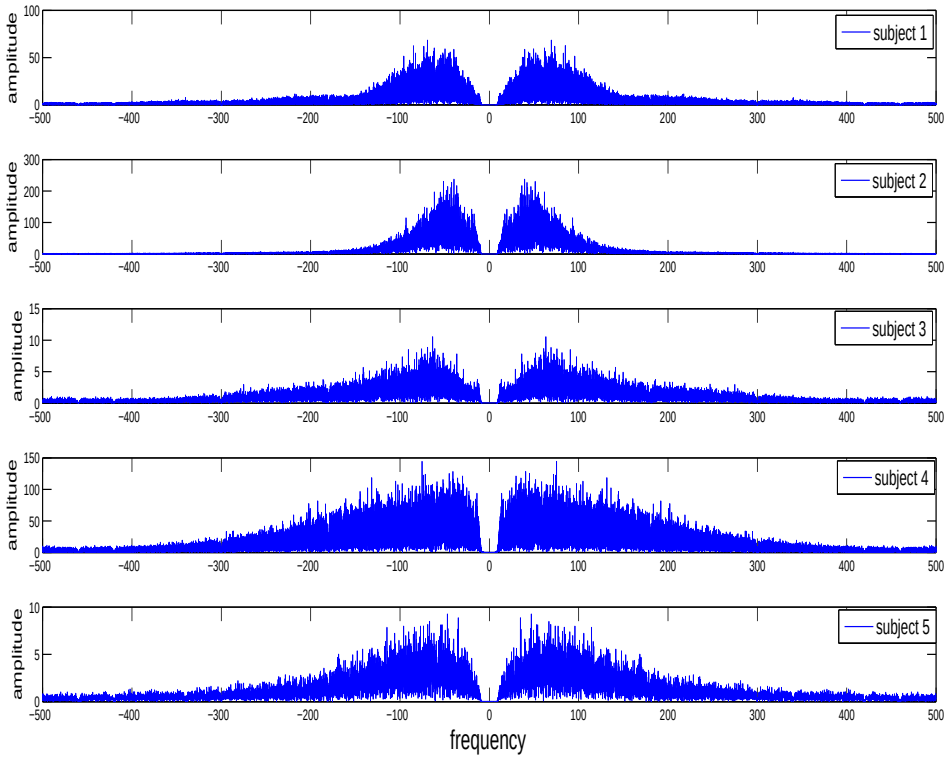

Figure 5.5: Isometric contraction after preprocessed signal of FT for all subjects

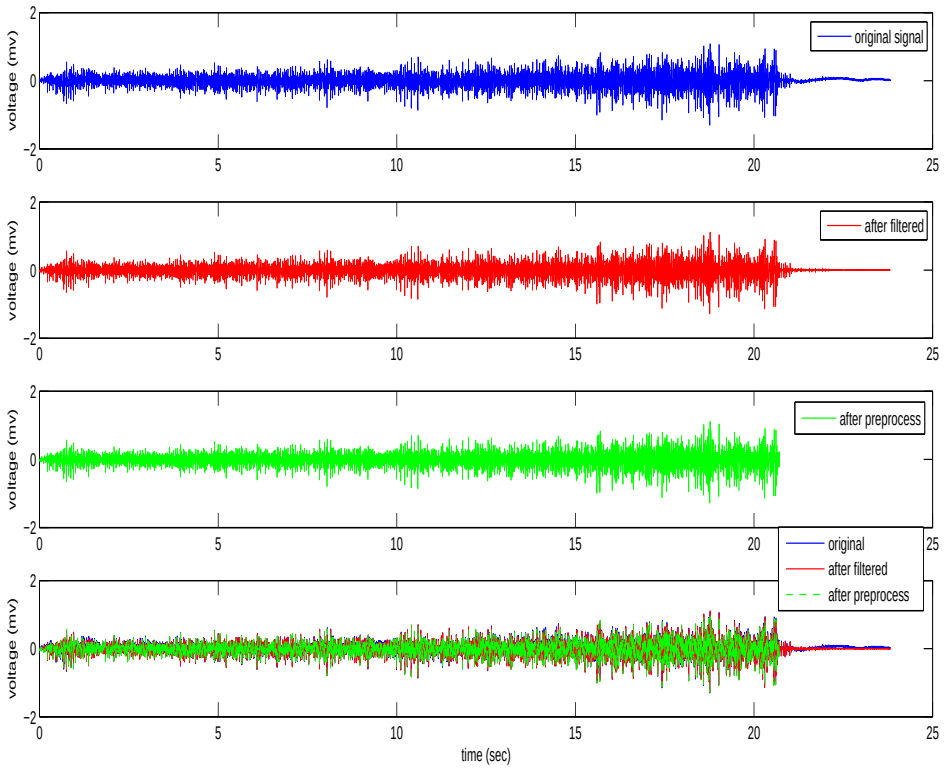

Figure 5.6: Signal after pre-process each step for subject 2

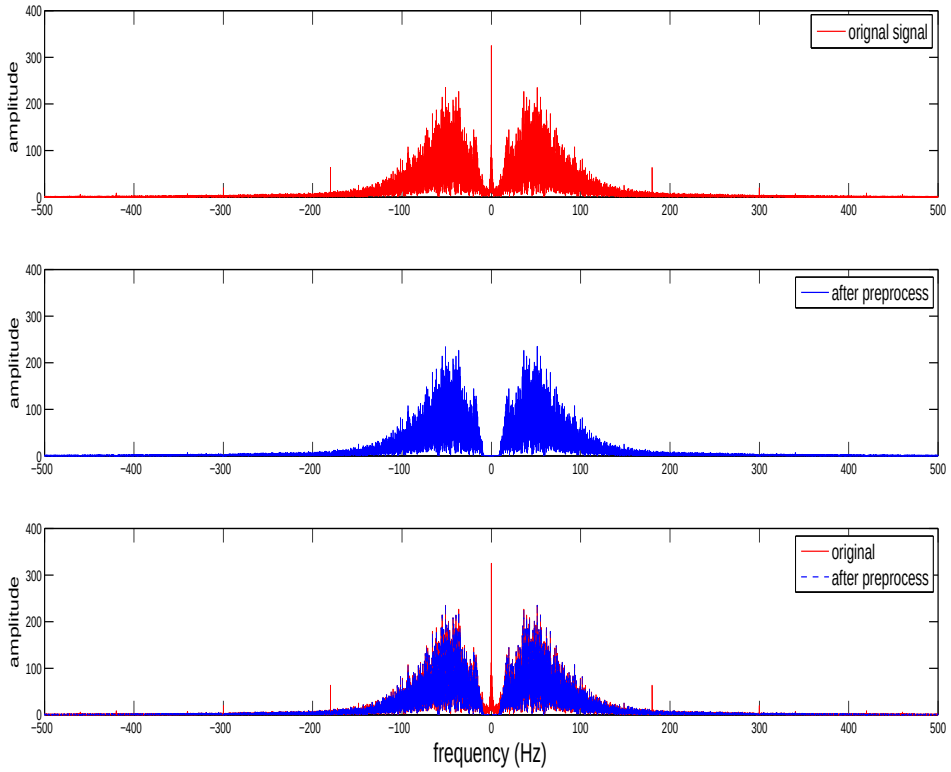

Figure 5.7: FT signal of after pre-process each step for subject 2

After filtering, the data was divided into several segments of the same length for running the MPD algorithm to avoid memory overload. The length of the segments is different from subject to subject because the time of exercise was different for each subject. The sEMG signal can be written as

$$x(t) = \sum_{i=0}^{L-1} x_i(t) \tag{5.2}$$

where $x_i(t) = x(t)((u(t - iT) - u(t - (i + 1)T))$ and T, the duration of each segment, here assumed constant. The energy of each segment was calculated and is summarized in Table 5.1. The energy of segment i is given by

$$E_{x_i} = \sum_{n=0}^{N-1} |x(nT_s)|^2, \tag{5.3}$$

where T_s is the sampling period and N is number of samples in a segment. The maximum energy indicated in bold in Table 5.1, was used to determine a threshold value for stopping the MPD algorithm.

Sub. #	subject1	subject2	subject3	subject4	subject5
segment 1	5.00×10^{-3}	1.37×10^{-1}	2.05×10^{-4}	5.01×10^{-2}	1.60×10^{-3}
segment 2	8.80×10^{-3}	2.32×10^{-1}	3.35×10^{-4}	6.06×10^{-2}	$\mathbf{1.70}\times10^{-3}$
segment 3	8.60×10^{-3}	$\mathbf{5.72}\times10^{-1}$	3.08×10^{-4}	7.75×10^{-2}	
segment 4	1.21×10^{-2}		5.40×10^{-4}	1.06×10^{-1}	
segment 5	$\mathbf{1.41}\times10^{-2}$		$\mathbf{5.44}\times10^{-4}$	1.06×10^{-1}	
segment 6	1.58×10^{-2}		2.96×10^{-4}	1.23×10^{-1}	
segment 7	2.23×10^{-2}		5.43×10^{-4}	$\mathbf{1.28}\times10^{-1}$	

Table 5.1: Energy for each segment for all subjects during isometric contraction

The MPD algorithm creates a dictionary, computing a projection of signal onto every Gaussian atom in the dictionary, selecting the dictionary atom $g_i(t)$ that has the maximum magnitude of the projection, calculating coefficient α_i and calculating a residue. The residue is compared to the threshold. If the energy of the

residue is greater than the threshold, the residue signal is then projected to the dictionary. The process continues with each iteration until the energy of the residue is less than the threshold. The diagram of the MPD algorithm summarizing all the steps is shown in Figure 5.8. For this study, the maximum and minimum frequencies in the dictionary were set 497.5 and 2.5 Hz respectively. Another parameter for selecting the dictionary is maximum and minimum scale. The scale, σ, of the Gaussian atom as shown in Figure 4.1. The maximum and minimum scale were set to be 0.2 and 600, respectively. These values were determined by trial and error and set both the isometric and dynamic contractions. MPD threshold values were set at 5% of maximum energy (bolded in Table 5.1) and 1% of maximum energy(bolded in Table 5.1) to compare the effects of threshold value. There is not much difference between the threshold 5% of maximum and 1% of maximum in MPD approximation and the corresponding MPD-TFRs are shown in Figure 5.9 (a)-(c), respectively. The 5% maximum segment of energy as a threshold was used for all subjects.

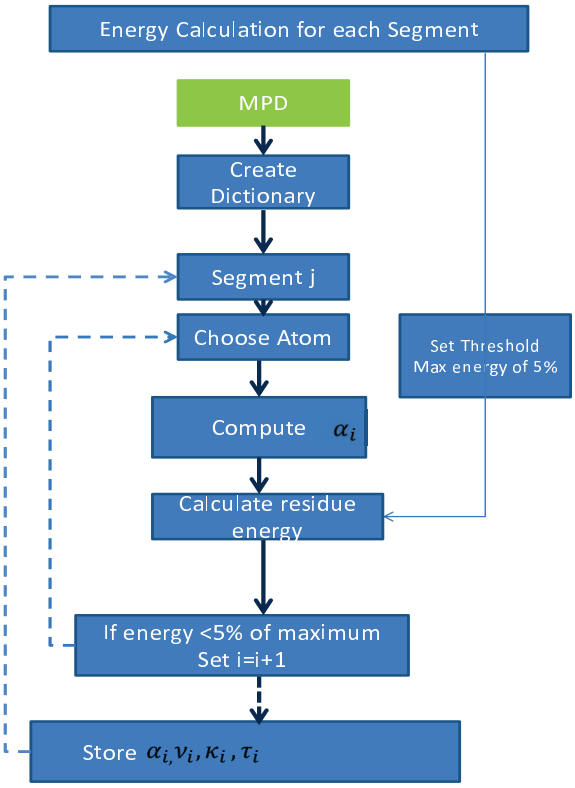

Figure 5.8: MPD algorithm

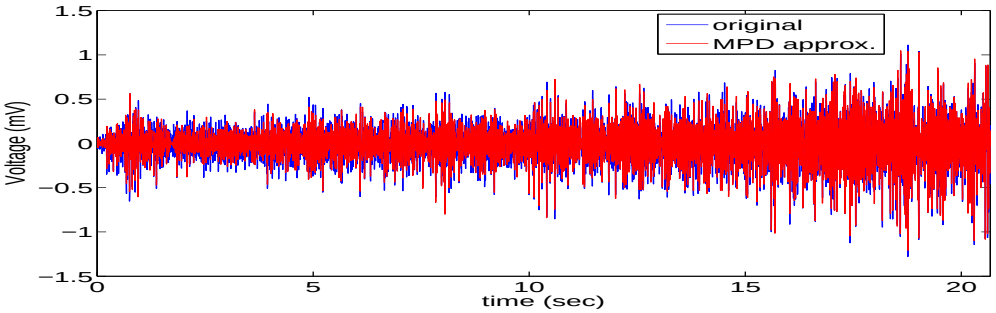

(a) MPD approximation with 5%max energy threshold

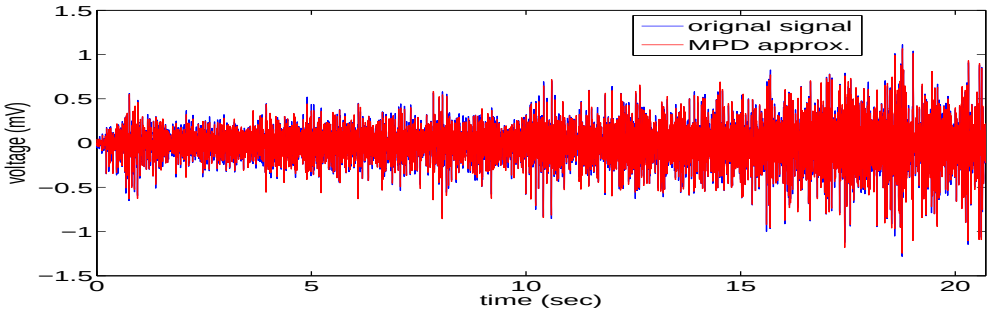

(b) MPD approximation with 1%max energy threshold

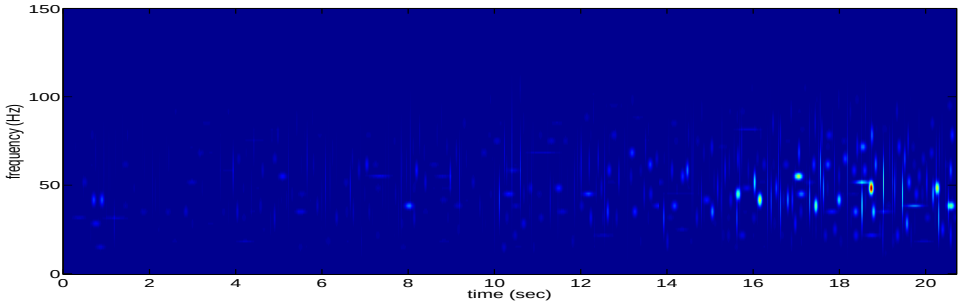

(c) MPD-TFR with 5%max energy threshold

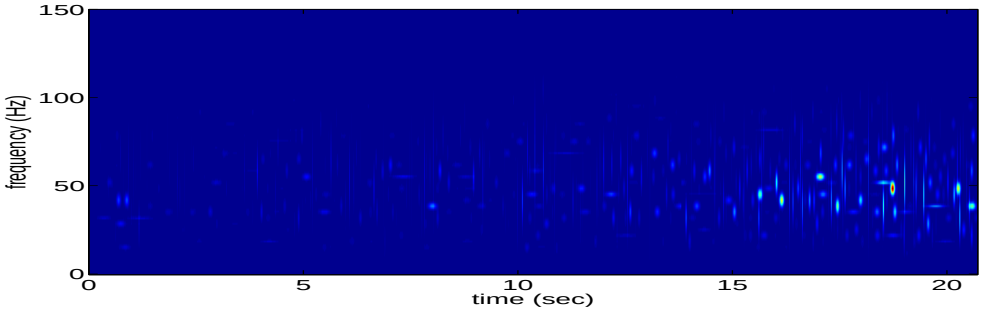

(d) MPD-TFR with 1%max energy threshold

Figure 5.9: MPD approximation and MPD-TFR with 1% and 5% maximum energy threshold during isometric contraction for subject 2.

The resulting vector of the time shift and frequency shift parameters and coefficients are plotted in three-dimensions as shown in Figure 5.10 (a). Modified WAIF as average of frequency was computed by using unique time-frequency feature vectors as described in Sectoion 5.1.1. The threshold that was used for stopping the MPD algorithm, was set to extract most information of the original sEMG signal so there were numerous data points. To reduce the amount of data without affecting the result, a second threshold, based on the coefficient value, was applied to calculate the modified WAIF in the data analysis phase to minimize the data required to describe fatigue. To extract the representation of the signal with fewer data points, several thresholds (see Figure 5.10(b)) for coefficient values were applied.

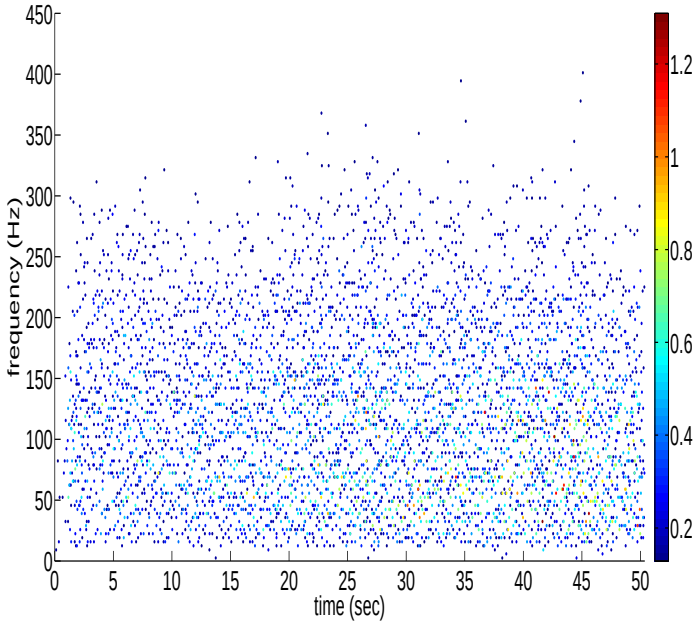

(a) Time vs. frequency with coefficient plot for isometric contraction for subject 4

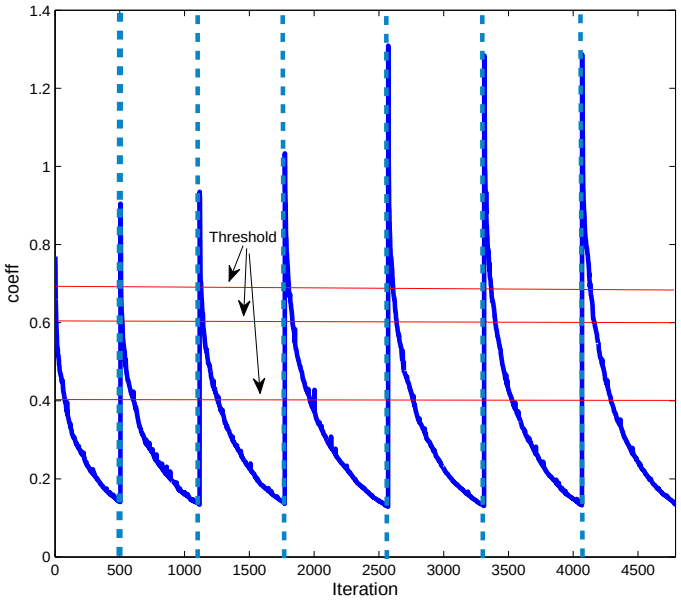

(b) Thresholds for coefficient value to calculate modified WAIF

Figure 5.10: Thresholds for coefficient value to calculate modified WAIF

The Figure 5.11 shows the result of the modified WAIF with the second thresholds, 0, 0.4, 0.6 and 0.7 and different interval lengths, 1, 1.5, 2, 2.5, and 3 seconds. The modified WAIF with threshold, 0.7 did not have enough data in the initial exercise to calculate the WAIF as shown in Figure 5.11(h). When the threshold value is larger, the number of data points is reduced. Different lengths of windows were applied to determine the optimum window length. From these data points, only one point at each frequency was chosen by picking the frequency that has a higher coefficient. Using a window length of 2.5 seconds shows a smoother result but also a similar trend to other window lengths as shown in Figure 5.11. The modified WAIF with a 2.5 second window length was evaluated for different thresholds. Linear regression was applied to find the trend of the slope using JMP. The relative change for each linear regression line was calculated as well. A spectrogram using a Gaussian window with window size 75 ms, 1 s, and 3.6 s without overlap was computed and then the IMNF (3.3) and IMDF in Equation(3.3) were computed. The relative change for each linear regression of IMNF and IMDF was calculated using MATLAB.

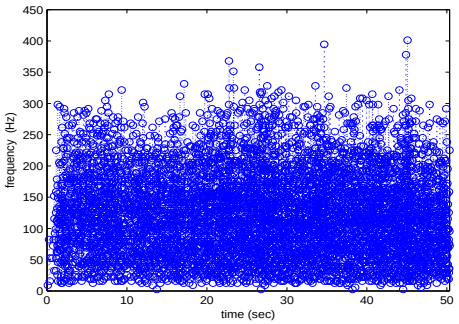

(a) threshold=0

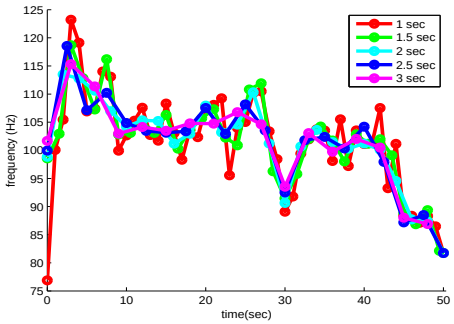

(b) Modified WAIF for threshold=0

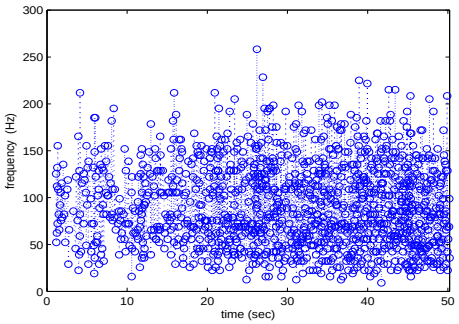

(c) threshold=0.4

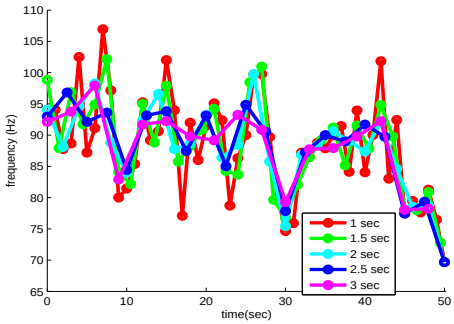

(d) Modified WAIF for threshold=0.4

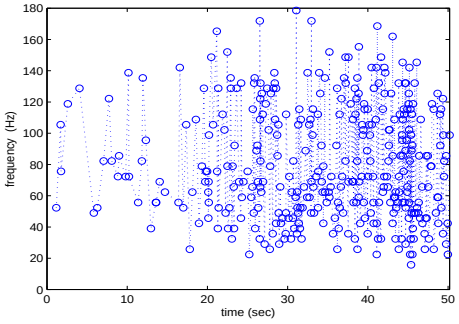

(e) threshold=0.6

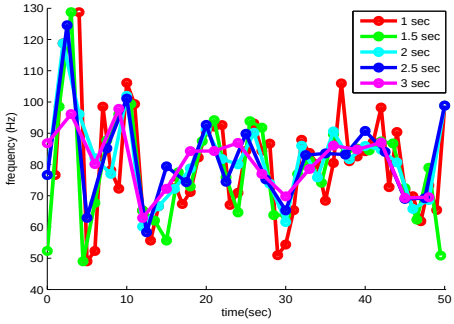

(f) Modified WAIF for threshold=0.6

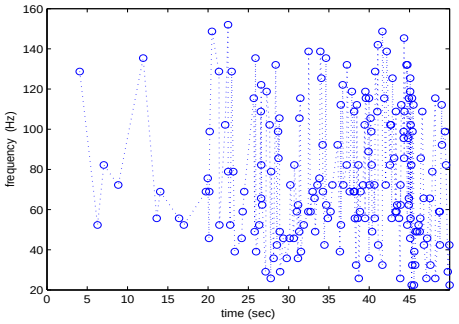

(g) threshold=0.7

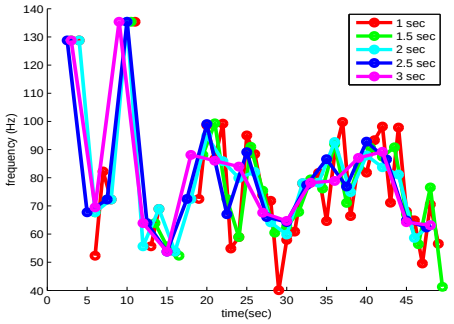

(h) Modified WAIF for threshold=0.7

Figure 5.11: Result of modified WAIF during isometric contraction for subject 4. It was computed with different thresholds and different computing windows, 1, 1.5, 2. 2.5 and 3 seconds.

5.3 Dynamic contraction data analysis

The original data of sEMG signal for dynamic contraction shows 60 Hz noise and DC offset. For the analysis of dynamic contractions, the preliminary signal preprocessing was the same as for the isometric contractions giving a signal for the exercise portion from 10 Hz to 500 Hz. The 60 Hz power line interference was removed as shown in Figure 5.12 in time domain and Figure 5.13 in the frequency domain for subject 5. The original signal processed signals for all subjects are shown in figure 5.14 and figure 5.16 respectively. The FT of the same signals for all subjects are shown in figure 5.15 and figure 5.17.

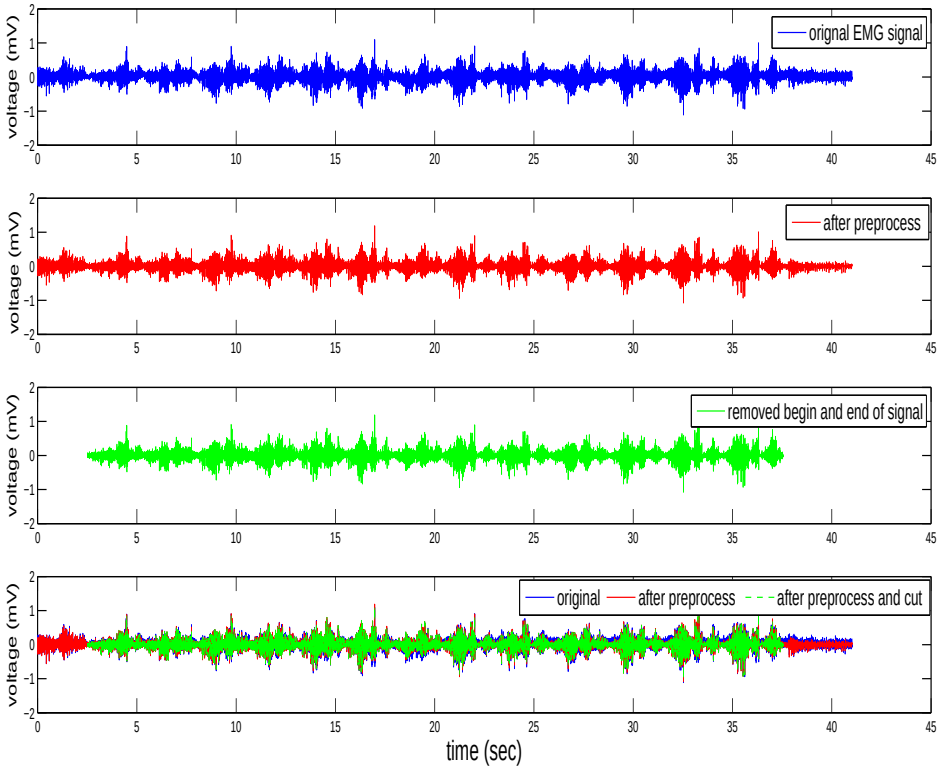

Figure 5.12: Dynamic contraction preprocessing in time domain for subject 5

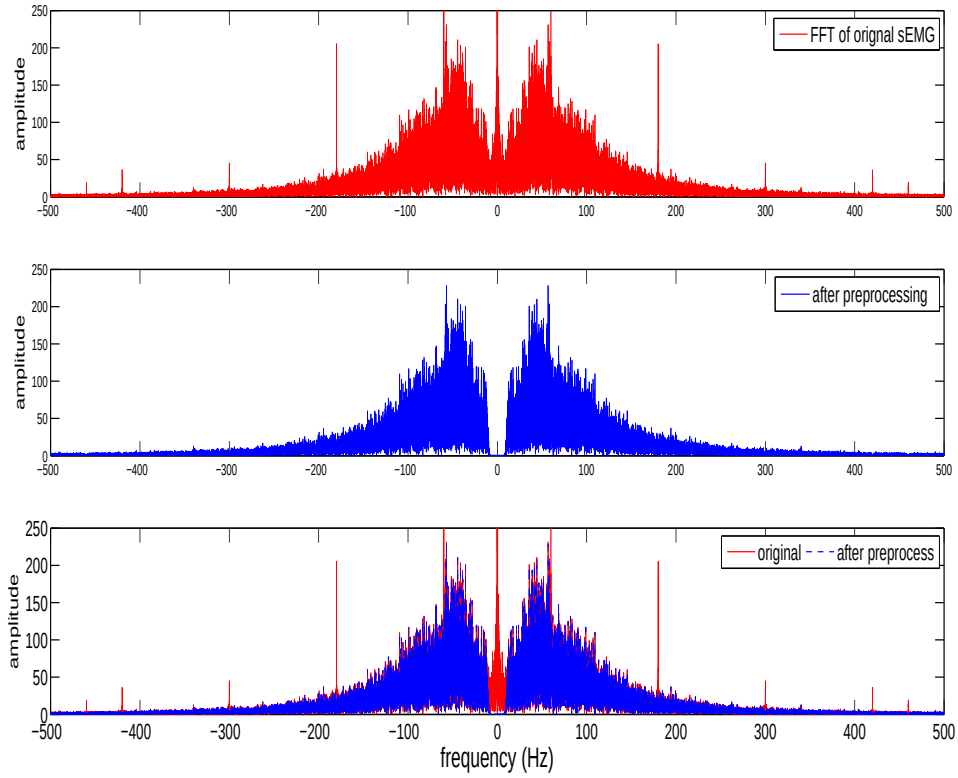

Figure 5.13: Dynamic contraction preprocessing in frequency domain for subject 5

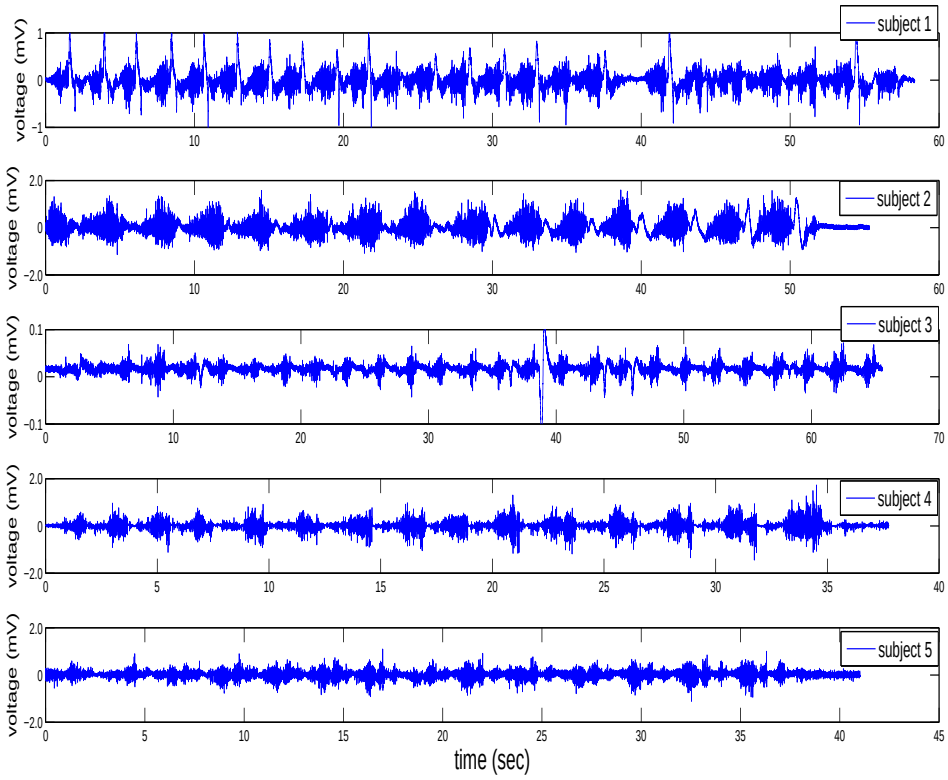

Figure 5.14: Dynamic contraction original signal for all subjects

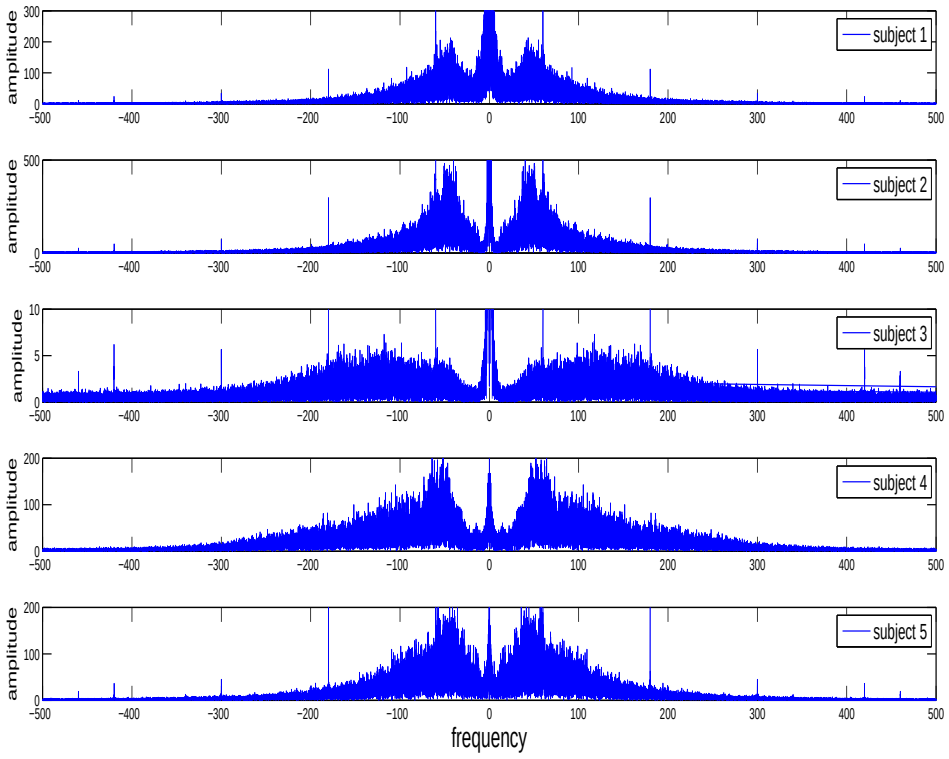

Figure 5.15: Dynamic contraction original signal of FFT for all subjects

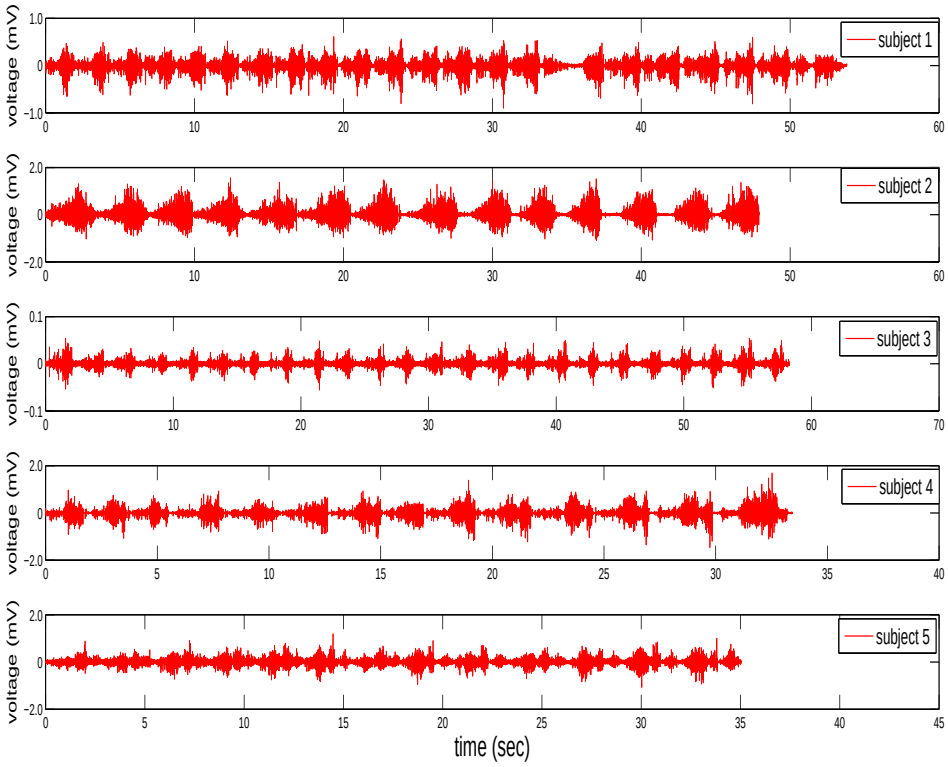

Figure 5.16: Dynamic contraction sEMG signal after preprocessed for all subjects

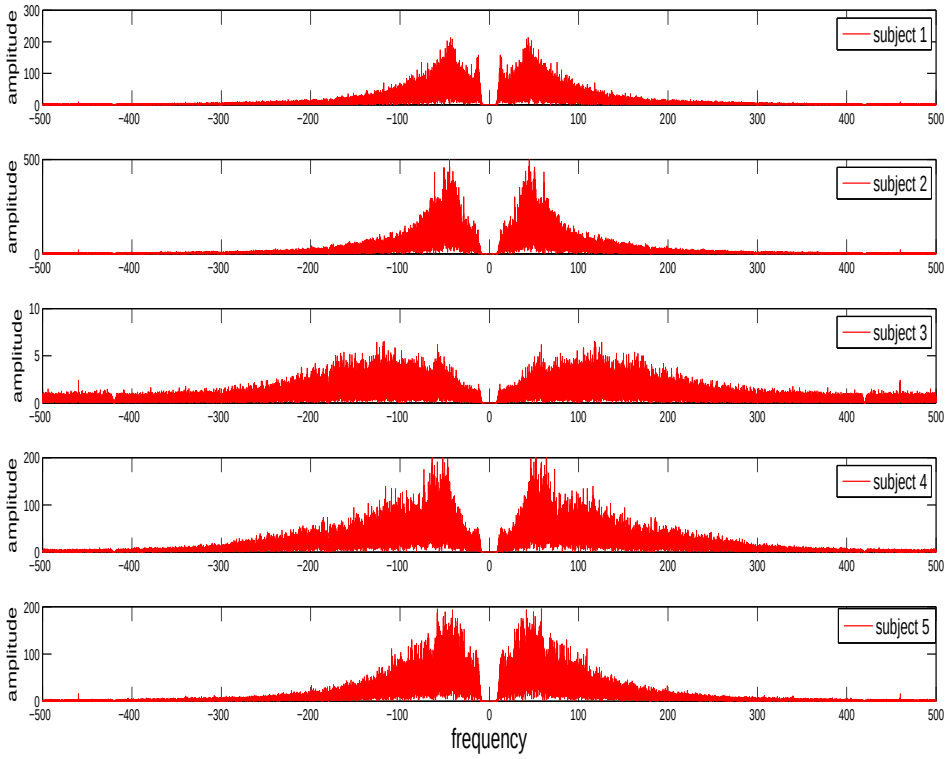

Figure 5.17: Dynamic contraction FFT of signal after preprocessed for all subjects

A cycle of sEMG signal, which is defined as moving a dumbbell up and back down, was determined manually, and it is shown in Figure 5.18 and Figure 5.19 for subject 2 and subject 4, respectively as an example.

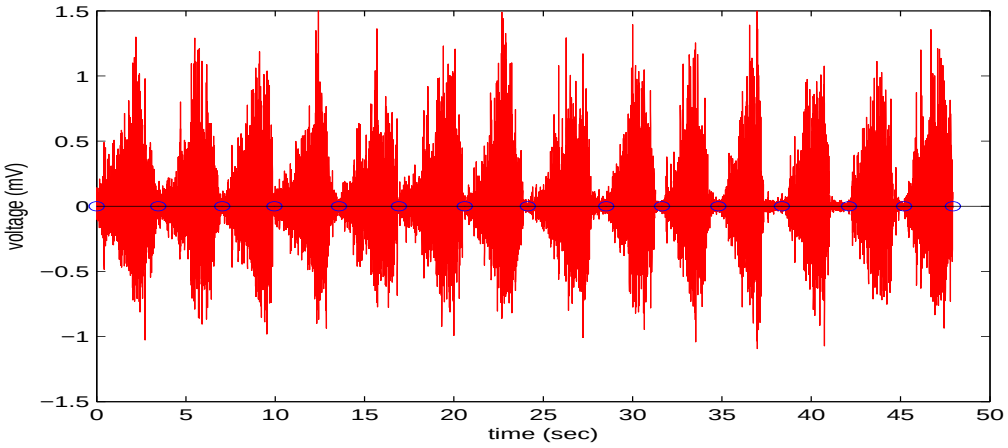

Figure 5.18: Each cycle of dynamic contraction for subject 2

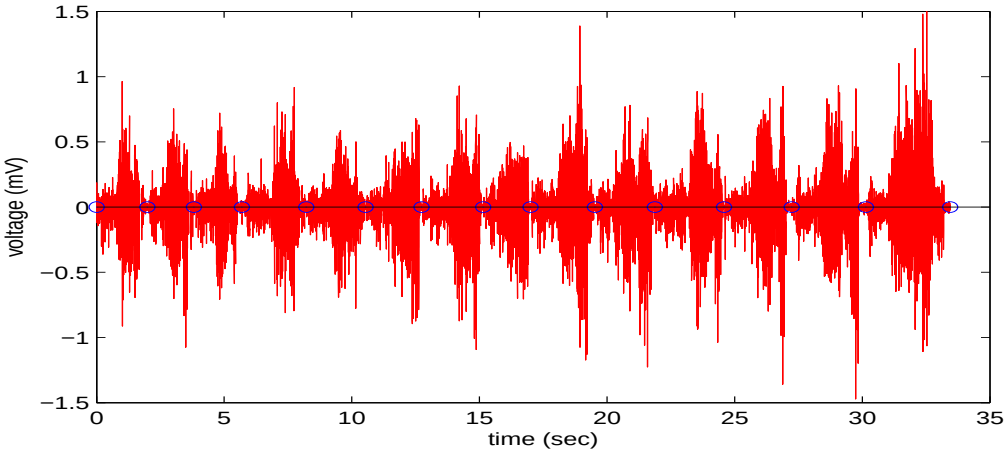

Figure 5.19: Each cycle of dynamic contraction for subject 4

The energy for each cycle was calculated and the maximum energy among them was used to set the threshold for the MPD. Table 5.2 shows the energy for each cycle for all subjects. The maximum is indicated in bold. 1% and 5% of the maximum energy was applied to determine a threshold for the MPD using subject 2 data. The MPD approximation of sEMG signal with a threshold value of the 5% of maximum energy does not extract information at edge cycles as shown in Figure 5.21.

The threshold was set to be 1% of maximum energy for all subjects during dynamic contraction as shown in Figure 5.21.

subject#	1	2	3	4	5
cycle 1	2.31×10^{-2}	2.04×10^{-1}	1.17×10^{-1}	4.08×10^{-2}	3.16×10^{-2}
cycle 2	2.78×10^{-2}	2.31×10^{-1}	4.91×10^{-2}	3.52×10^{-2}	3.67×10^{-2}
cycle 3	2.55×10^{-2}	2.26×10^{-1}	5.48×10^{-2}	2.75×10^{-2}	6.12×10^{-2}
cycle 4	2.56×10^{-2}	1.96×10^{-1}	2.93×10^{-2}	4.67×10^{-2}	5.67×10^{-2}
cycle 5	2.82×10^{-2}	1.82×10^{-1}	5.51×10^{-2}	3.34×10^{-2}	6.95×10^{-2}
cycle 6	2.95×10^{-2}	2.48×10^{-1}	4.74×10^{-2}	5.13×10^{-2}	8.00×10^{-2}
cycle 7	2.47×10^{-2}	2.48×10^{-1}	4.74×10^{-2}	6.55×10^{-2}	3.69×10^{-2}
cycle 8	3.49×10^{-2}	2.38×10^{-1}	5.35×10^{-2}	4.66×10^{-2}	6.89×10^{-2}
cycle 9	3.72×10^{-2}	2.07×10^{-1}	7.57×10^{-2}	8.15×10^{-2}	5.53×10^{-2}
cycle 10	2.57×10^{-2}	2.18×10^{-1}	5.65×10^{-2}	7.32×10^{-2}	5.07×10^{-2}
cycle 11	3.64×10^{-2}	1.95×10^{-1}	$\mathbf{4.70}\times10^{-1}$	7.57×10^{-2}	7.34×10^{-2}
cycle 12	2.75×10^{-2}	2.39×10^{-1}	5.72×10^{-2}	9.19×10^{-2}	8.58×10^{-2}
cycle 13	$\mathbf{3.89}\times10^{-2}$	1.98×10^{-1}	5.06×10^{-2}	1.06×10^{-1}	$\mathbf{1.06}\times10^{-1}$
cycle 14	3.85×10^{-2}	1.60×10^{-1}	8.20×10^{-2}	$\mathbf{1.92}\times10^{-1}$	
cycle 15	3.66×10^{-2}	$\mathbf{2.24}\times10^{-1}$	7.61×10^{-2}		
cycle 16	3.08×10^{-2}		5.16×10^{-2}		
cycle 17	3.02×10^{-2}		8.17×10^{-2}		
cycle 18	3.25×10^{-2}		6.94×10^{-2}		
cycle 19	3.23×10^{-2}		6.64×10^{-2}		
cycle 20	3.62×10^{-2}		7.02×10^{-2}		
cycle 21	2.79×10^{-2}		6.39×10^{-2}		
cycle 22	2.27×10^{-2}		8.52×10^{-2}		
cycle 23			1.26×10^{-1}		
cycle 24			7.43×10^{-2}		

Table 5.2: Energy for each cycle for all subjects during dynamic contraction

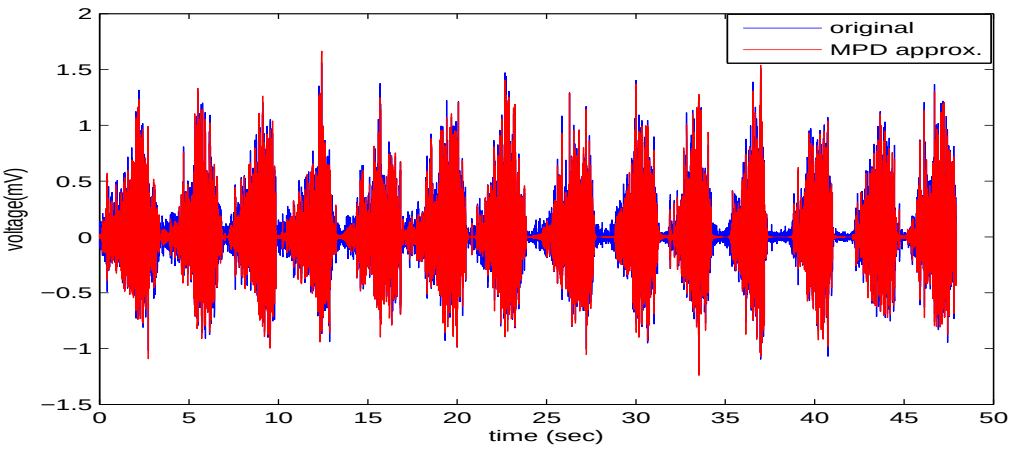

Figure 5.20: MPD approx signal with threshold 95% for subject 2

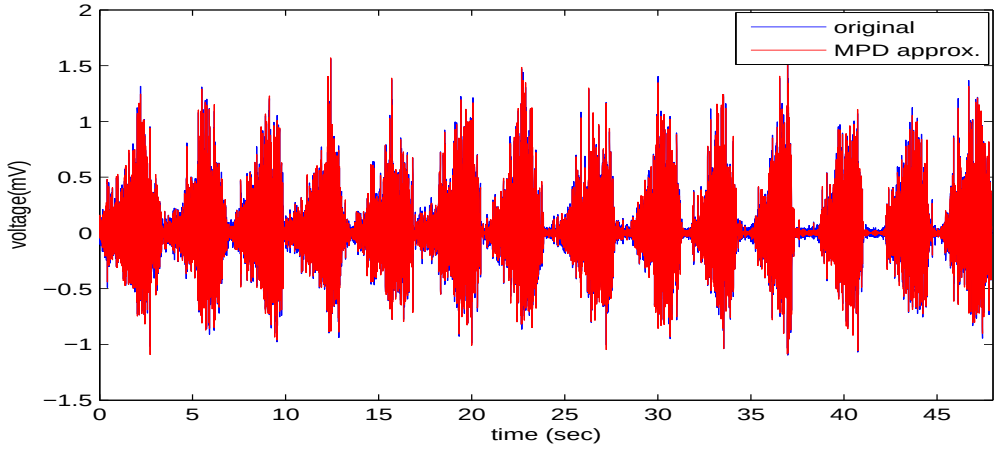

Figure 5.21: MPD approx signal with threshold 99% for subjet 2

We used our MPD algorithm as before for isometric contractions except the threshold value was now set 1% of the maximum energy. MPD was run for each cycle to avoid memory overload. The moodified WAIF was calculated for each cycle with a second threshold which was selected based on the values o the coefficients. The modified WAIF was applied to detect changes in frequency with respect to time. The slope and initial frequency of the modified WAIF for different second thresholds were determined by linear regression using JMP. A spectrogram using a Gaussian

window with four different durations 75 ms, 500 ms, 1000 ms and 2000 ms, was computed for subject 1, 2, and 5. For subject 3 and 4, the Gaussian window varied between 75 ms, 500 ms, 1000 ms and 1800 ms because the duration of the cycle time was shorter than 2 seconds. The IMNF in (3.3) and IMDF in (3.4) were obtained from the spectrogram. Over the cycle, IMNF and IMDF were averaged and linear regression was computed over the whole exercise to see the trend in frequency. The relative change of each linear regression was calculated for all subjects.

Chapter 6

RESULTS AND DISCUSSION OF RESEARCH STUDY

6.1 Experimental Process for sEMG Measurements

6.1.1 Study Participants

Five subjects were selected from the general population of healthy persons between the ages of 21 and 60 years old on campus at Arizona State University. This study was approved by the Arizona State University IRB. Persons with a history of neuromuscular impairment were excluded as were body builders to insure that the data more closely matched the general population. The sEMG signals were recorded from the dominant hand biceps brachii for the constant force isometric contraction and from the non-dominant hand biceps brachii for dynamic contractions. The participates signed a consent form.

6.1.2 Equipment Used in the Experiment

The instrumentation used was the BIO PAC Systems HLT 100C, ISP100C, and EMG100C to collect the EMG signals. The following parameters were used for processing:

- Sampling frequency 1000 Hz
- Lowpass filter 500 Hz
- Highpass filter 1.0 Hz
- Notch filter off

Bio-Pac EL254RT silver-silver chloride electrodes were used for this study. The size of the electrode is 7.2 mm outer diameter and has a 4 mm recording diameter. The EMG gel used in the study was Signagel GEL1.

6.1.3 Experimental Data Collection Process

This experimental data was recorded at the Biomechatronics LAB at Arizona State University. Subjects were asked if they were currently experiencing fatigue in their upper body to insure that data was collected for a non fatigue condition. Subjects were told that they can stop anytime for any reason. The skin surrounding the biceps brachii of the dominant hand was cleaned with rubbing alcohol. The electrodes were placed with conductive EMG gel. The distance between electrodes was about 5 to 7mm. A ground connection was made to the skin over the distal end of the radius. First, the sEMG signal was recorded with the subject relaxing with no muscle contraction for 10 seconds. Next, the maximum of the sEMG signal was measured for the maximum voluntary contraction (MVC) for the dominant arm by having the subject push up with a maximum force from underneath the table for about 5 second and rest for about 5 seconds. This cycle was repeated 3 times. After this initial evaluation, the subject rested to recover from the MVC. The subject held a dumbbell (15 lb for female and 25 lb for male) in the dominant hand with elbow flexed at a 90 degree angle and held that position until the subject could no longer hold the weight. After this, the constant force isometric contraction was recorded, the electrodes were removed and the conductive EMG gel was wiped off. Next, the electrodes were placed with conductive gel on the non-dominant side biceps brachii after the skin surrounding the biceps brachii was cleaned with rubbing alcohol. The sEMG signal was collected with the subject relaxing, no contraction, for 10 seconds. The MVC of the sEMG signal was measured for the non- dominant arm by having the subject push up with a maximum force on the underside of the table for about 5 seconds and rest for about 5 seconds. The cycle was repeated 3 times. After the subject was rested from the maximum voluntary contraction, the subject was asked to cyclically move his/her arm from 180 degree angle (extended elbow) through the

full range of motion (flexed elbow) until the upper arm was touching the upper body. This cycle was repeated until the subject could not lift the dumbbell further to complete a full cycle of extension and flexion. A metronome was used to guide the timing of the extension and flexion. The tempo of the metronome was adjusted to the individual's comfortable tempo. The summary of the information is shown below in the Table 6.1.

subject #	Gender	time duration isometric contraction (sec)	time duration dynamic contraction (sec)	repetition for dynamic contraction
1	female	62.471	54.184	23
2	female	20.719	47.924	14
3	male	21.259	58.277	24
4	female	50.365	33.444	14
5	male	13.322	35.054	13

Table 6.1: Summary of Subject Information

6.2 MPD Processing of sEMG Signal from Isometric Contractions

The MPD approximation of the sEMG signals of isometric contractions for all subjects with the threshold set to be 5% of maximum energy gave a result very close to the orignal sEMG signal. The MPD approximation of the sEMG signal (red), and real sEMG signal (blue), were plotted together and the plots for subject 1 and subject 2 as examples are shown in a and b respectively in Figure 6.1 (a) and (b).

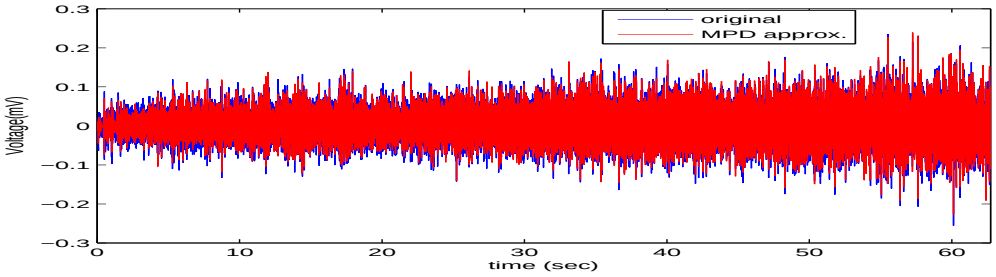

(a) subject 1

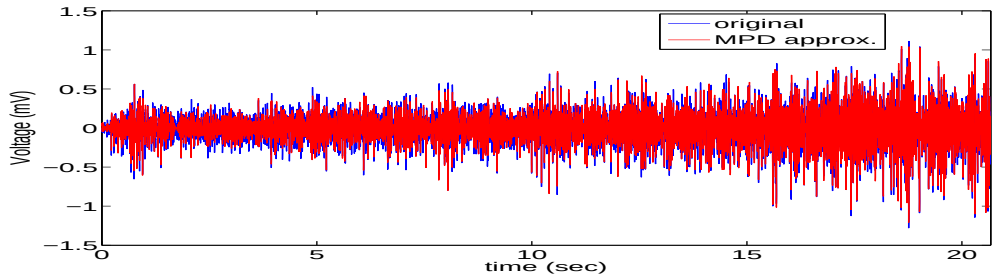

(b) subject 2

Figure 6.1: The MPD approximation of sEMG signal (red line) and real sEMG signal (blue line)was plotted together. (a) subject 1 (b) subject 2

The MPD-TFRs of the sEMG signals for all subjects are shown in Figure 6.2. MPD-TFRs were not normalized making direct comparison between subjects difficult. The range of frequency was from 40 to 300 Hz, depending on the subject. The range of amplitude also depended on the subject. Subject 1, subject 2, and subject 4 show higher amplitude at end of the signal. Subject 3 and subject 5

showed higher amplitudes in the middle and/or at the beginning of the signal. The highest amplitude can be seen very clearly for all subjects.

Spectrograms with a Gaussian window of duration 75 ms, 1 s, and 3.6 s, for subject 2, are shown in Figure 6.3. The window size affects the resolution of the spectrogram. According to the uncertainty principle in (3.7), the window size of the spectrogram affects the resolution of time and frequency domain. The effect of increasing the window duration causing the frequency resolution to decrease is demonstrated in Figure 6.3.

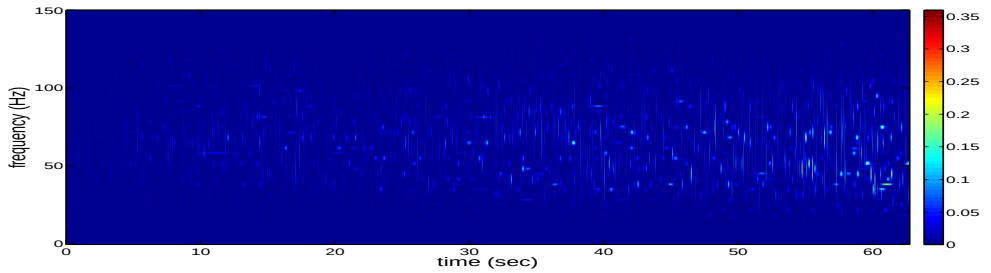

(a) subject 1

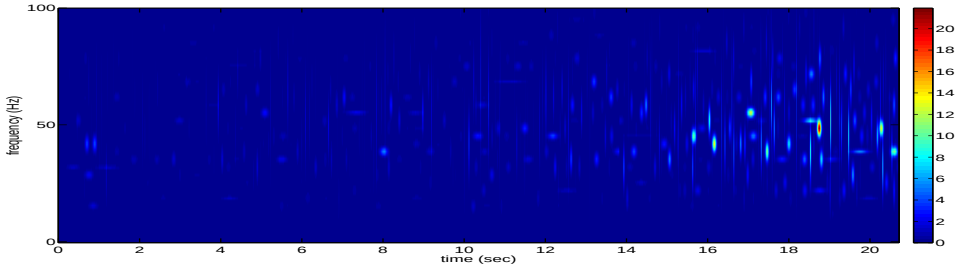

(b) subject 2

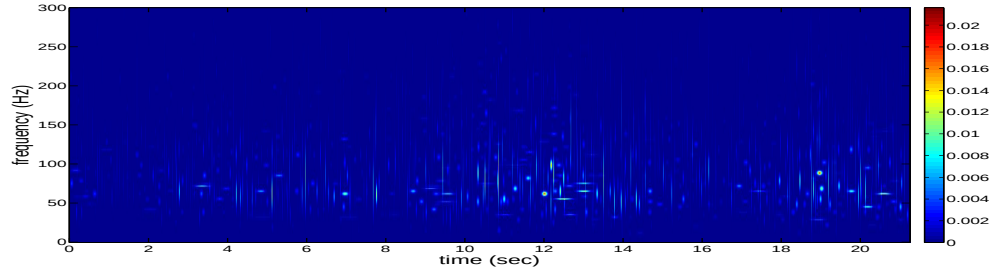

(c) subject 3

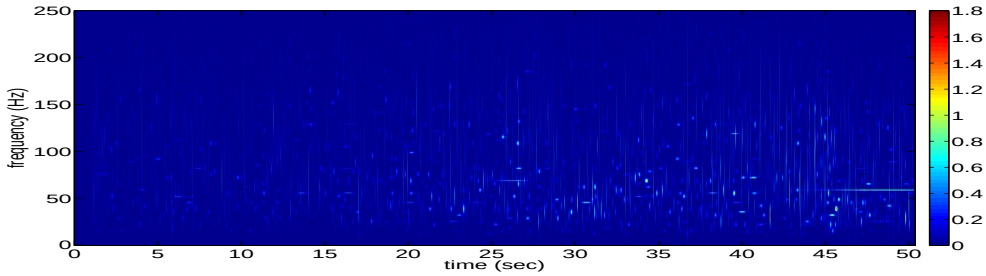

(d) subject 4

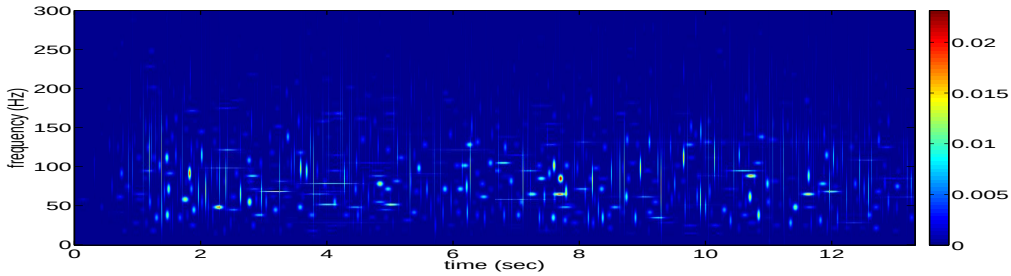

(e) subject 5

Figure 6.2: The MPD-TFR plots for Isometric contraction for all subjects

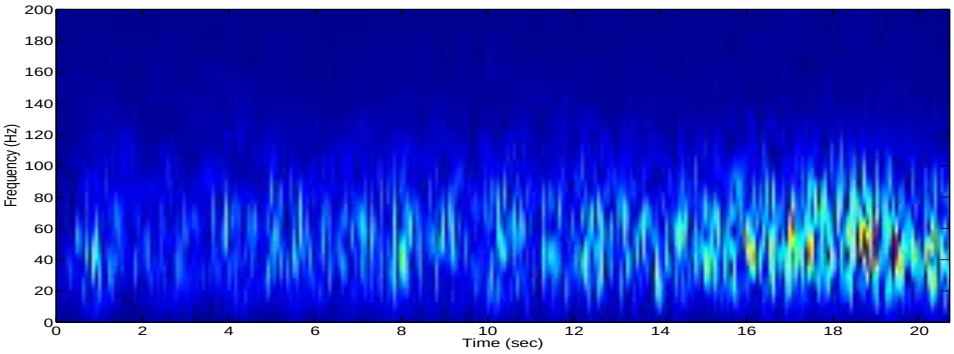

(a) Spectrogram with window size 75 ms

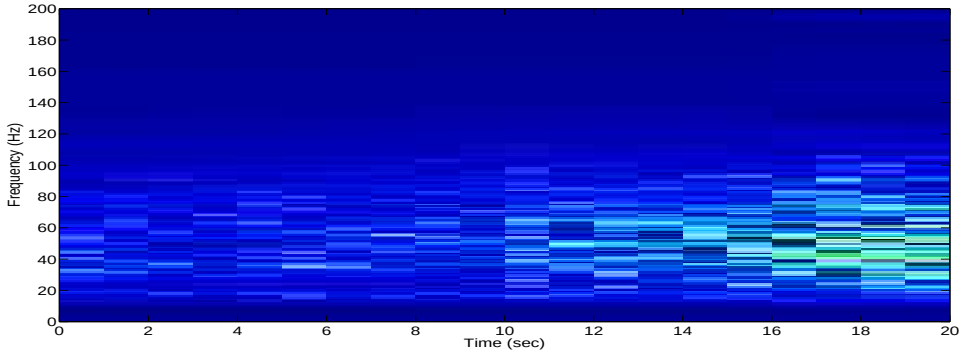

(b) Spectrogram with window size 1 s

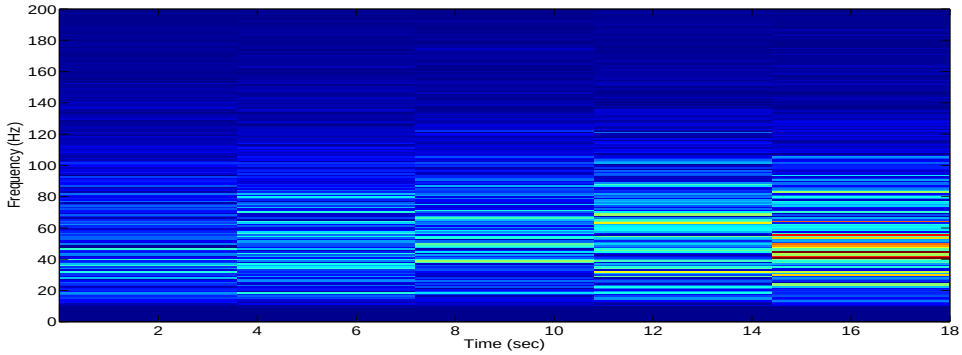

(c) Spectrogram with window size 3.6 s

Figure 6.3: Spectrogram with three different window sizes, 75 ms, 1s, and 3.6 s for subject 2

The number of data points was reduced by setting a threshold for selecting the coefficients. The MPD gives the coefficient, time shift, frequency shift and scale for each time-frequency points selected, as shown by the MPD-TFR in Figure 5.10(a). Several threshold coefficients were tested to see if the result could be obtained with fewer data points. When the threshold increased, the early time segment did not have enough points to compute the modified WAIF. The threshold value for the coefficient and number of thresholds depend on the subject. The plot of the modified WAIF and its linear regression line for subject 1, 2, and 3 are shown in figure 6.4. The plot of the modified WAIF and its linear regression line for subject 4 and 5 are shown in Figure 6.5. Table 6.2 displays the result of the modified WAIF for the slope (sl.), average of slope (Av. sl.), standard deviation of slope (Std.sl.), initial frequency (In.fr.), average initial frequency(Av.In.fr.), standard deviation of initial frequency (Std.fr.), R-square (R-sq.), relative change (Re.Ch(%)) and average of relative change (Av.Re.Ch.). The relative change was measured using a point at the beginning of the exercise and a point at the end to form the linear regression lines for all subjects for the isometric contraction. The modified WAIF for all subjects shows a negative slope. The modified WAIF with threshold equal to zero, resulted in the largest number of extracted components;the only components exclued had smaller coefficients when there multiple frequency points at the same time as described in Chapter 5.1.1. Comparing the modified WAIF with threshold 0 to ones with different thresholds, the same trend was observed with the trend lines approximately parallel for smaller coefficients. But, when the threshold was increased, beyond some limit, changes in the slope were observed. The relative change from the modified WAIF for subject 1, 2, and 5 reuslted in higher value as the threshold value increased.

	Thr	sl.	Av.sl.	Std.sl.	In.fr.	Av.In.fr.	Std.fr.	R-Sq.	Re.Ch(%)	Av.Re.Ch.
S1	0	-0.16	-0.17	0.01	75.04	72.70	1.81	0.45	27.79	31.58
	0.1	-0.17			73.18			0.52	28.37	
	0.15	-0.16			71.58			0.43	29.68	
	0.2	-0.18			71.00			0.37	40.48	
S2	0	-0.20	-0.36	0.18	54.63	55.35	1.91	0.43	6.90	12.11
	1	-0.22			53.18			0.51	5.97	
	1.25	-0.43			55.88			0.85	13.35	
	1.5	-0.58			57.69			0.64	22.22	
S3	0	-0.43	-0.30	0.19	105.10	100.58	6.40	0.44	12.79	11.84
	0.02	-0.17			96.05			0.09	10.89	
S4	0	-0.46	-0.38	0.12	113.63	104.45	12.98	0.65	31.05	29.54
	0.4	-0.29			95.27			0.41	28.02	
S5	0	-0.66	-0.59	0.21	103.53	93.42	8.93	0.76	9.67	9.85
	0.04	-0.35			90.12			0.60	5.58	
	0.06	-0.77			86.61			0.57	14.30	

Table 6.2: The result of modified WAIF for constant isometric contraction. Thr=threshold.

For the spectrogram, the IMNF in (3.3) and the IMDF in(3.4) and their linear regression were computed. Plots for IMNF and IMDF for the different windows, 75 ms, 1 s, and 3.6 s and their linear regression lines for subject 2 and subject 5 are shown in Figure 6.6. Table 6.3 summarizes the IMNF results and Table 6.4 summarizes the IMDF result. Both tables show slope and initial frequency (In.fr.) with R-square (R-Sq) and relative change (Re. Ch(%)) of the linear regression line as measured between the beginning of the exercise and the end for all subjects for isometric contraction. The slopes for the IMNF and IMDF show negative except for the IMDF for subject 5. This possitive slope was obserbed for a window size, 3.6 ms which is shown in figure 6.6 (b). The result of IMNF and IMDF got decreased as the window size increased loosing information for the early part of the cycle.The relative change decreased as the window size in increased for all subjects. Overall, the IMNF showed higher range than IMDF and this could be due to the fact that the IMNF is sensitive to force output [1].

	W. size	Slope	In. fr.	R-Sq	Re. Ch(%)
subject 1	75 ms	-0.43	141.04	0.27	19.22
	1000 ms	-0.41	140.77	0.77	17.92
	3600 ms	-0.40	139.89	0.94	16.45
subject 2	75 ms	-0.76	91.20	0.22	17.18
	1000 ms	-0.97	94.87	0.72	19.43
	3600 ms	-0.69	91.41	0.74	10.96
subject 3	75 ms	-0.80	170.02	0.10	9.88
	1000 ms	-0.80	170.26	0.41	9.89
	3600 ms	-0.96	169.42	0.47	8.29
subject 4	75 ms	-0.34	156.95	0.09	10.90
	1000 ms	-0.38	160.87	0.37	11.57
	3600 ms	-0.34	161.06	0.53	9.10
subject 5	75 ms	-0.84	162.73	0.05	6.88
	1000 ms	-1.16	166.98	0.42	8.35
	3600 ms	-0.52	163.58	0.41	2.28

Table 6.3: Result of the IMNF for constant isometric contraction. W. size is window size.

	W. size	Slope	In. fr.	R-Sq	Re. Ch(%)
subject 1	75 ms	-0.29	99.29	0.12	18.28
	1000 ms	-0.27	97.47	0.47	16.90
	3600 ms	-0.23	96.11	0.91	13.68
subject 2	75 ms	-0.34	65.06	0.04	10.72
	1000 ms	-0.52	67.56	0.35	14.70
	3600 ms	-0.49	66.50	0.43	10.71
subject 3	75 ms	-0.76	134.96	0.05	11.93
	1000 ms	-0.83	135.26	0.32	12.31
	3600 ms	-1.00	133.84	0.43	10.71
subject 4	75 ms	-0.37	131.84	0.05	13.96
	1000 ms	-0.40	136.89	0.29	14.48
	3600 ms	-0.27	134.09	0.24	8.83
subject 5	75 ms	-0.50	125.86	0.01	5.17
	1000 ms	-0.85	128.29	0.21	8.05
	3600 ms	**0.41**	121.83	0.25	-2.37

Table 6.4: Result of the IMDF for constant isometric contraction. W. size is window size.

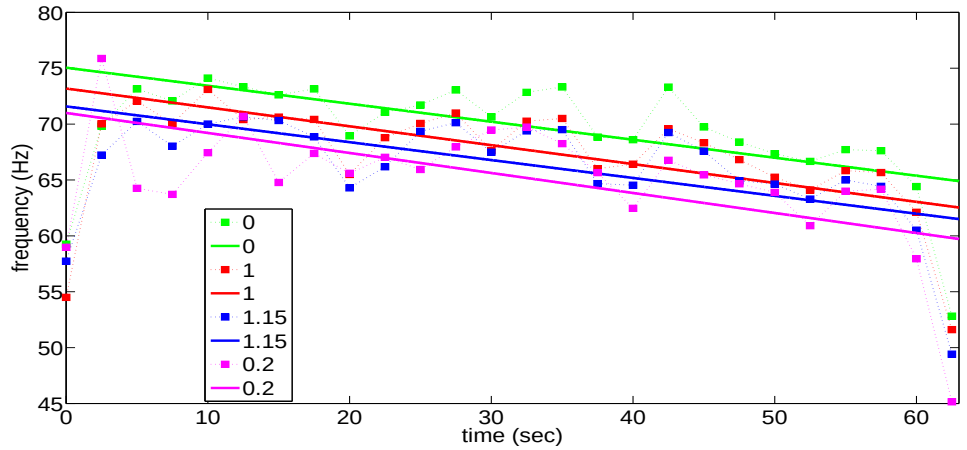

(a) subject 1

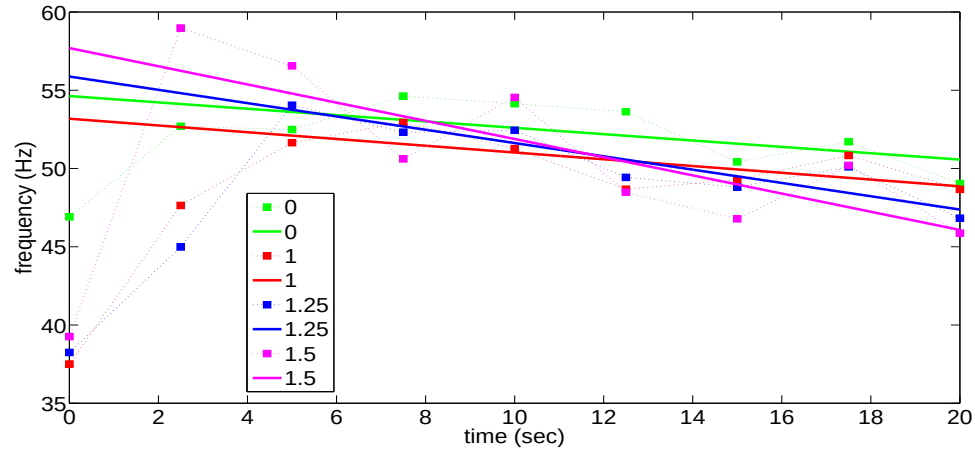

(b) subject 2

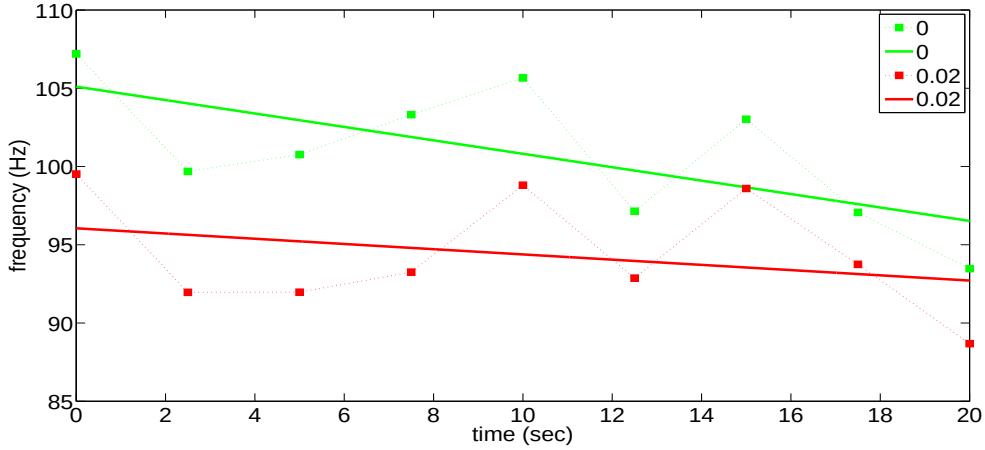

(c) subject 3

Figure 6.4: Modified WAIF for different coefficients (dot) with linear regression lines (solid line) for subject 1, 2, and 3 during isometric contraction

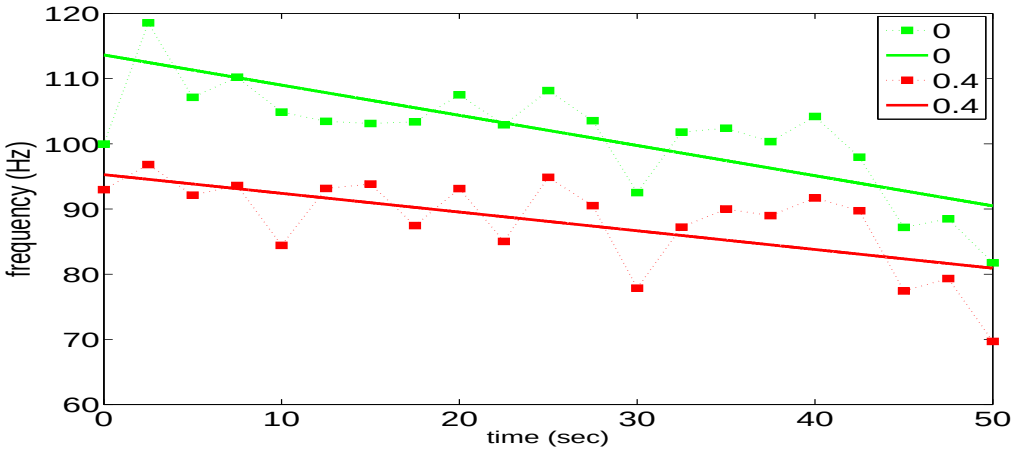

(a) subject 4

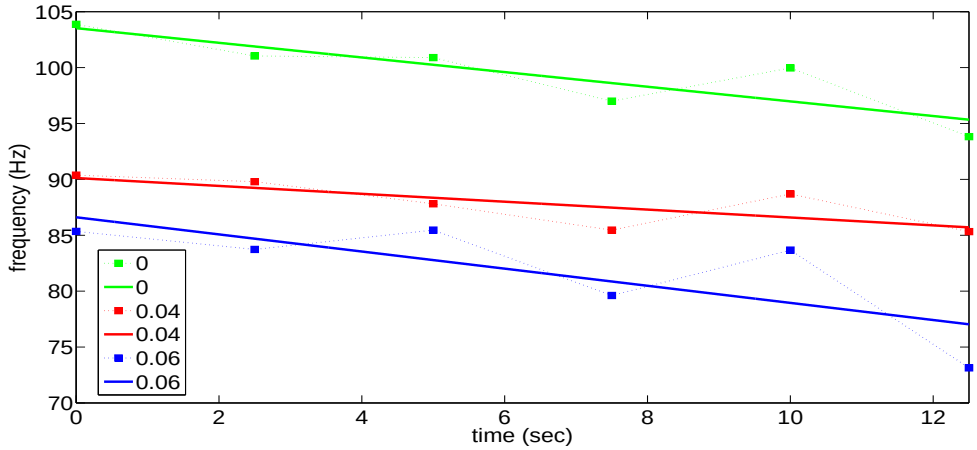

(b) subject 5

Figure 6.5: Modified WAIF for different coefficients (dot) with linear regression lines (solid line) for subject 4 and 5 during isometric contraction

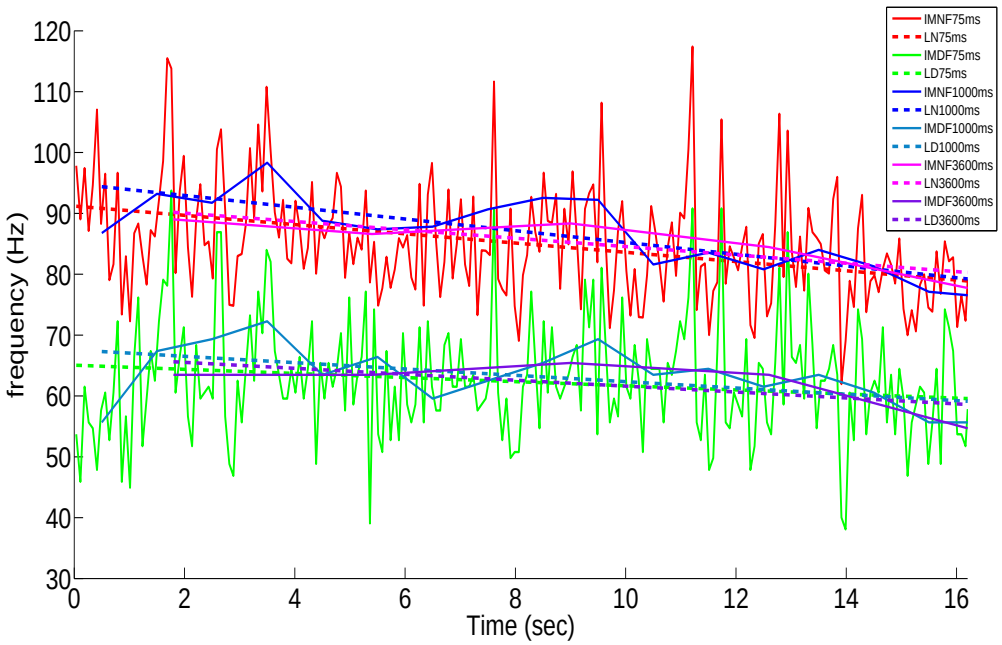

(a) subject 2

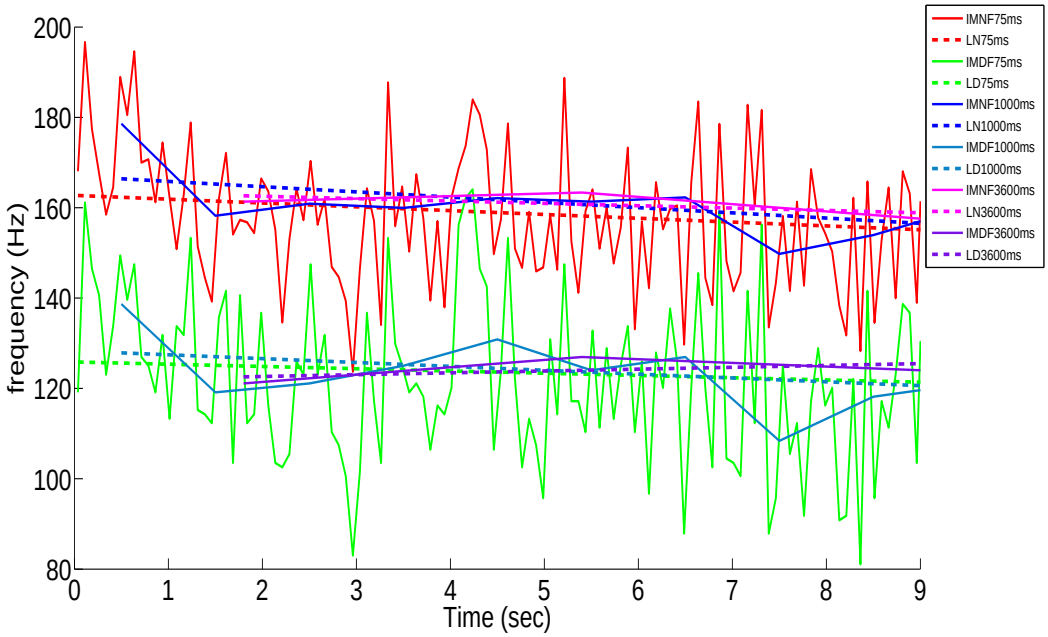

(b) subject 5

Figure 6.6: Spectrogram for different windows with linear regression lines for subject 2 and 5 for isometric contraction

6.3 MPD Processing of sEMG Signals from Dynamic Contraction

The MPD approximation of the sEMG signals of dynamic contractions for all subjects with the threshold set to 1% of the maximum energy gave a result very close to the orignal sEMG signal. The MPD approximation of dynamic contraction of the sEMG signal using the 5% threshold of the maximum energy did not adequately extract signal information as shown in Figure 5.21. The MPD approximation of the sEMG signal, the red line, and the real sEMG signal, the blue line, were plotted together for subject 2 and subject 4 are shown in Figure 6.7 (a) and (b) respectively. MPD-TFR plots for each cycle from the beginning (cycle 1) of the exercise sequence to the end (cycle 14) for subject 4 are shown in Figure 6.8. Plots of the spectrograms with window size 75 ms and 1000 ms for subject 4 are shown in figure 6.9 and figure 6.10 respectively. As with isometric contractions, time resolution decreases as the window size increases.

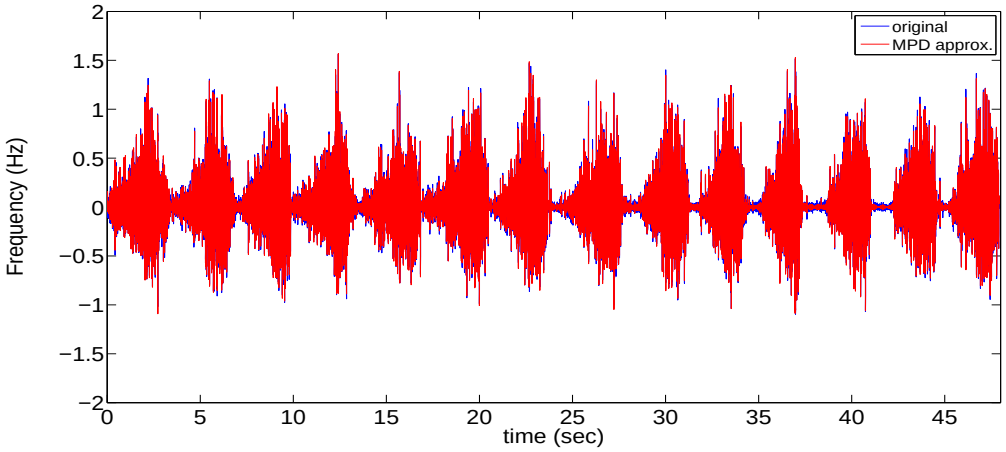

(a) subject 2

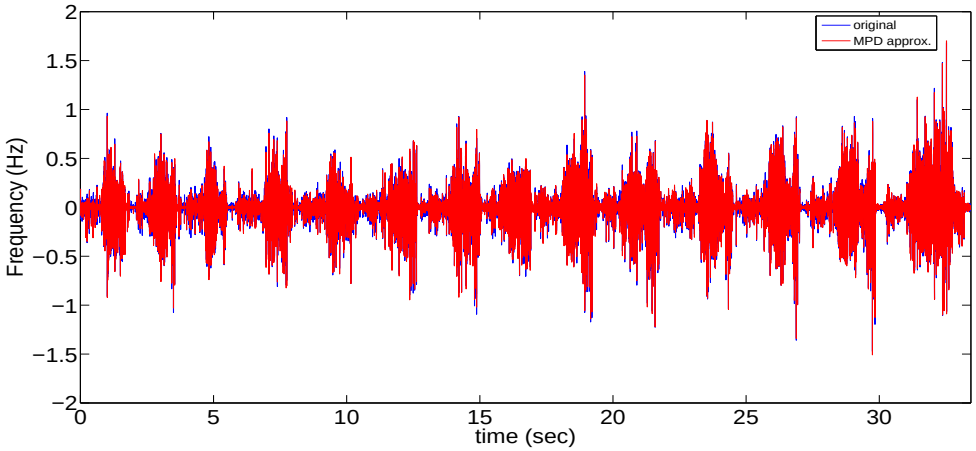

(b) subject 4

Figure 6.7: The MPD approximation of sEMG signal (red line) and real sEMG signal (blue line) for dynamic contraction was plotted together. (a) subject 2 (b) subject 4

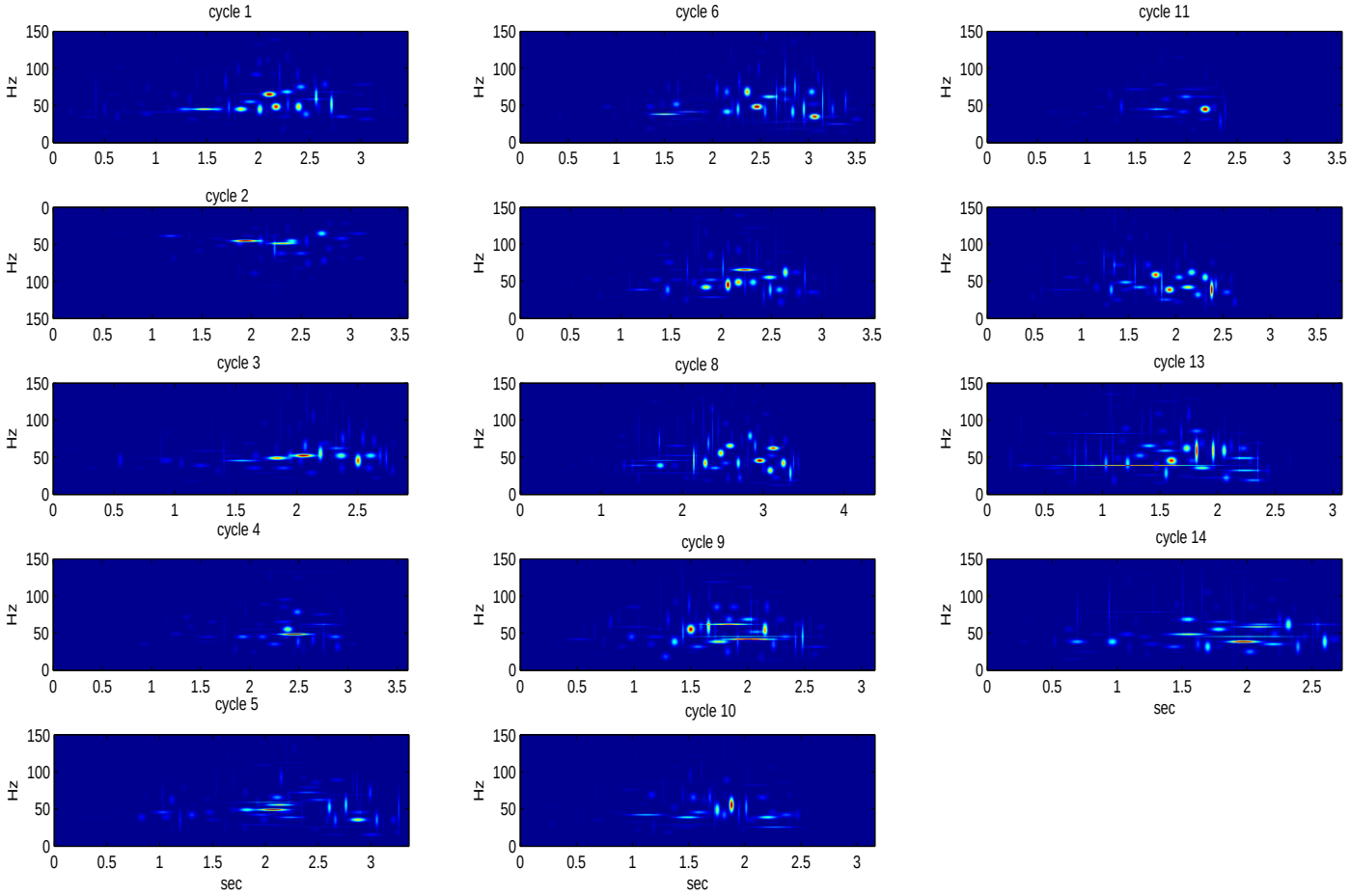

Figure 6.8: MPD-TFR for dynamic contraction for subject 4

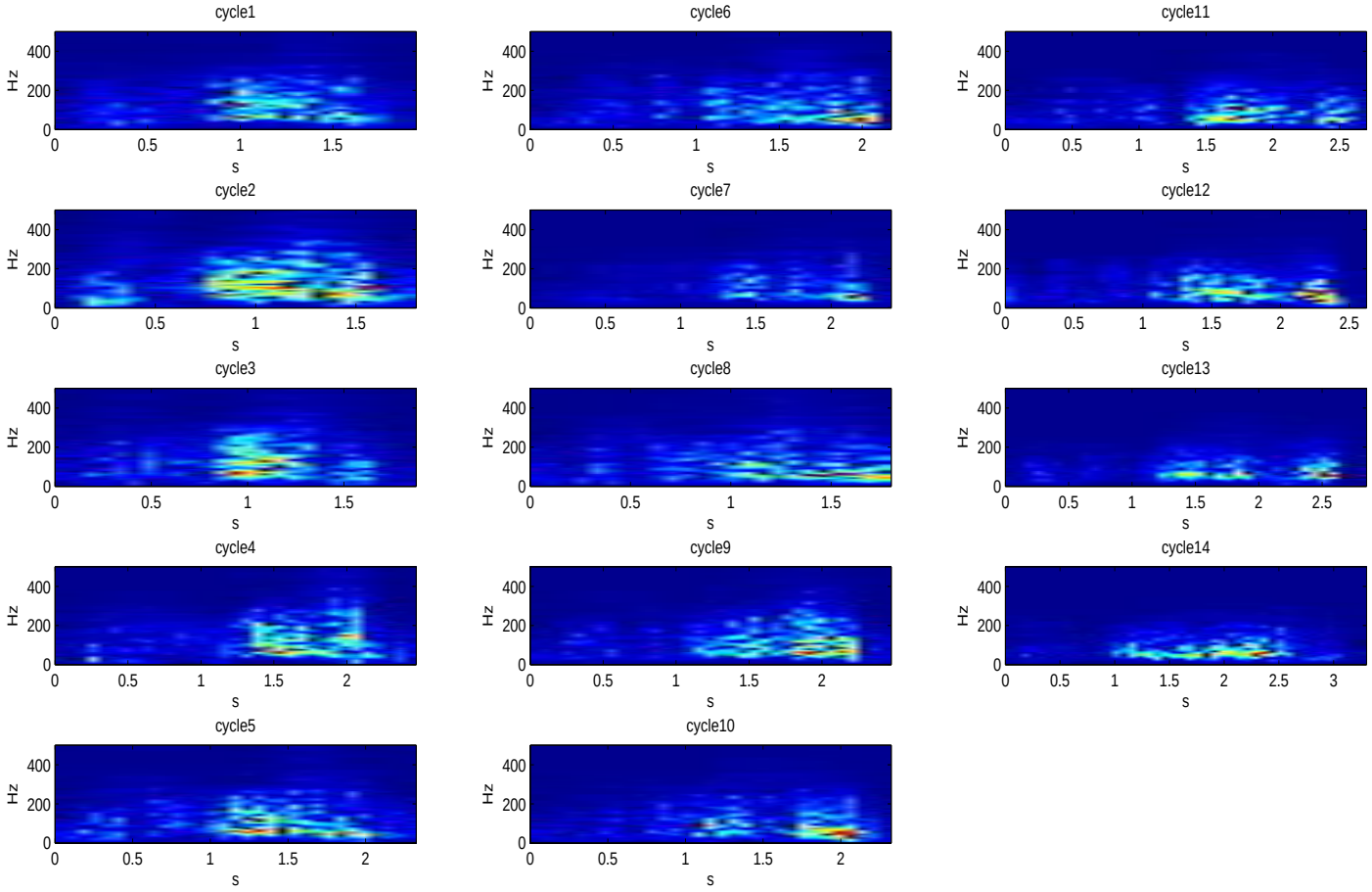

Figure 6.9: Spectrogram with Gaussian window 75ms for subject 4 during dynamic contraction

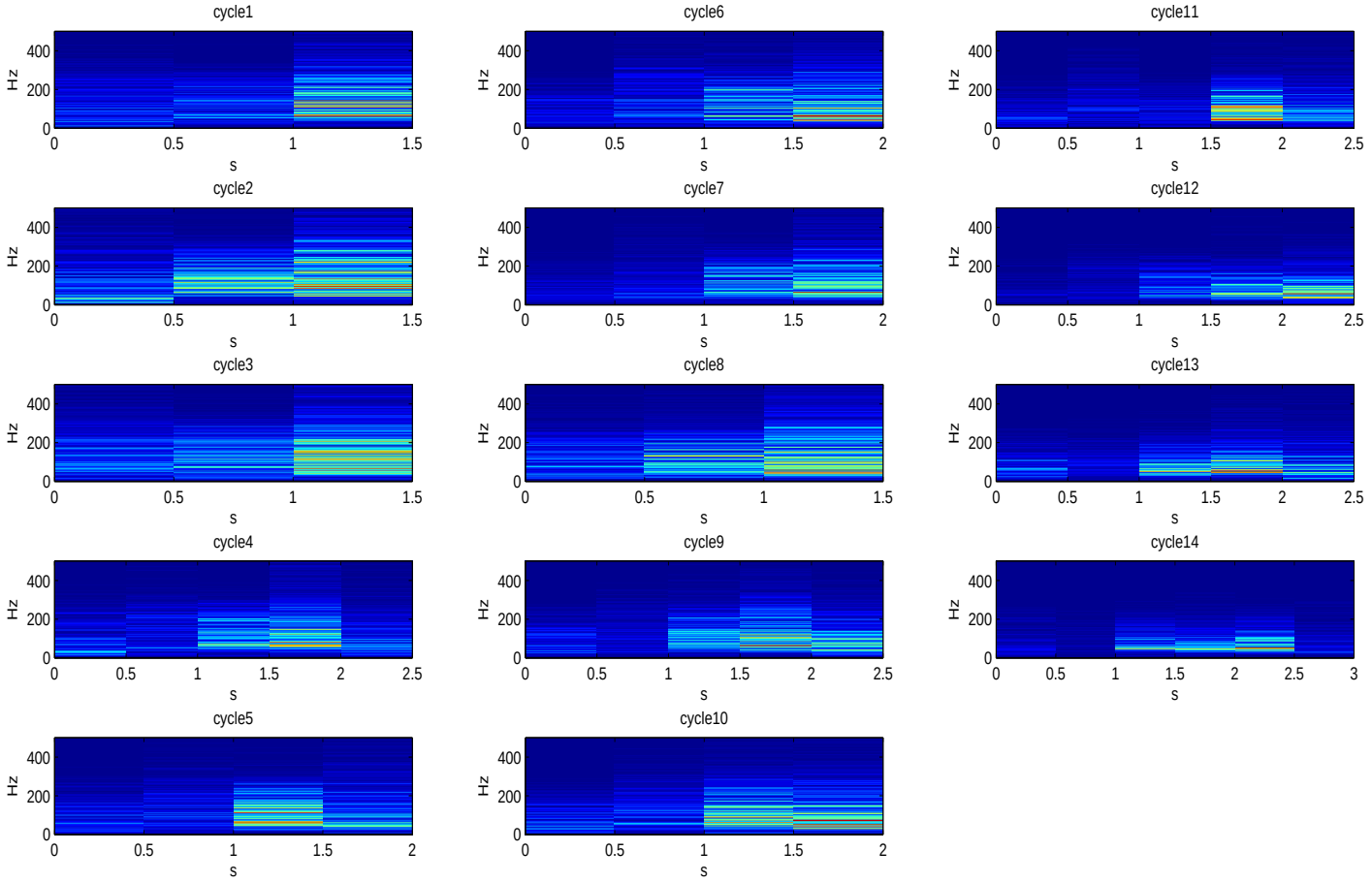

Figure 6.10: Spectrogram with Gaussian window 500ms for subject 4 during dynamic contraction

The modified AWIF for each cycle with different coefficient thresholds was calculated. All results show a negative slope as exercise progressed. The frequency and time data set was reduced by setting a threshold coefficient. For dynamic contractions, the threshold was increased systematically to determine how many data points could be eliminated before the trend became distorted. The threshold value depends on the subject. Subject 4 and subject 5 had the same threshold. The plot of the modified WAIF and linear regression lines for all subjects are shown from Figure 6.11 to Figure 6.15. Increasing the threshold did not change the linear regression of the frequency change trend, but the frequency was overall lower. The range of the initial frequency showed 50 Hz to 70 Hz for subject 1, subject 2, and subject 5. The rest of the subjects had a higher range, 90 Hz to 170 Hz. Table 6.5 summarizes the modified WAIF with slope (sl.), average slope (Av.sl), standard deviation of slope (Std.sl.) initial frequency (In.fr.), average of initial frequency (Av.In.fr.), standard deviation of frequency (Std.fr.) and R-square (R-Sq). The relative change (%)of slope as measured from the start to the end of the exercise and the average relative changes are shown in table 6.6. Subject 1 and subject 3 showed increasing relative change (%) as the threshold values increased. The relative change (%) decreased as the threshold value increased for the rest of the subjects. However, the changes in trends of decreasing relative change are very small compared to changes where an increase was observed.

	Thr	Sl.	Av.sl.	Std.sl.	In.fr.	Av.In.fr.	Std.fr.	R-Sq.
sub 1	0	-0.25	-0.23	0.02	61.71	53.27	5.18	0.66
	0.5	-0.20			54.20			0.50
	0.75	-0.21			51.91			0.41
	1	-0.24			50.06			0.31
	1.25	-0.22			48.45			0.15
sub 2	0	-0.12	-0.11	0.02	59.84	54.29	3.34	0.60
	1	-0.12			54.91			0.61
	2	-0.13			52.96			0.69
	2.5	-0.08			51.93			0.38
	3	-0.09			51.83			0.22
sub 3	0	-0.49	-0.41	0.06	158.94	144.02	10.47	0.54
	0.01	-0.41			143.56			0.51
	0.02	-0.38			137.60			0.41
	0.03	-0.35			135.97			0.28
sub 4	0	-1.65	-1.43	0.21	125.40	113.82	11.50	0.88
	0.25	-1.53			123.17			0.85
	0.5	-1.54			116.36			0.78
	0.75	-1.32			105.72			0.69
	1	-1.14			98.47			0.55
sub 5	0	-0.50	-0.37	0.11	74.33	66.37	6.28	0.79
	0.25	-0.42			70.27			0.79
	0.5	-0.41			66.96			0.69
	0.75	-0.24			60.96			0.55
	1	-0.29			59.33			0.42

Table 6.5: The result of modified WAIF for dynamic contraction. Thr is threshold value.

	Threshold	Relative Change(%)	Average Relative Change
subject 1	0	41.73	44.99
	0.5	24.54	
	0.75	34.89	
	1	53.99	
	1.25	69.79	
subject 2	0	11.31	11.20
	1	11.16	
	2	13.27	
	2.5	9.59	
	3	10.68	
subject 3	0	18.08	18.90
	0.01	17.26	
	0.02	17.91	
	0.03	22.36	
subject 4	0	43.65	43.06
	0.25	43.95	
	0.5	42.69	
	0.75	42.79	
	1	42.22	
subject 5	0	24.57	21.00
	0.25	21.93	
	0.5	23.44	
	0.75	14.04	
	1	21.03	

Table 6.6: The relative change and average relative from the result of modified WAIF for dynamic contraction.

The slopes for linear regression of IMNF and IMDF are negative except for IMNF and IMDF with window size 2 seconds for subject 2. The summary of IMNF is in Table 6.7 including slope, initial frequency (In.fr), R-square (R-Sq), and relative change (%) (Re.Ch(%)) of slope as measured from the start to the end of the exercise. The summary of IMDF is in Table 6.8 including slope, initial frequency (In.fr), R-square (R-Sq), and relative change (%) (Re.Ch(%)) of slope as measured from the start to the end of the exercise. The range of initial frequency for IMDN for all subjects is from 100 Hz to 200 Hz. The relative change for IMNF showed an increasing trend only for subject 1 and subject 3. The range of intial frequency for IMDF for all subjects is from 60 Hz to 190 Hz. Overall, the IMDF is lower than IMNF. The relative change for IMDF showed that it increased when the window size increased for most subjects. The plots of IMNF and IMDF from the spectrogram for subject 2 and subject 5 for dynamic contraction are shown in Figure 6.16 and Figure 6.17 respectively.

	W size	Slope	In. fr.	R-Sq	Re.Ch(%)
subject 1	75 ms	-0.18	97.75	0.47	9.34
	500 ms	-0.32	101.85	0.62	15.97
	1000 ms	-0.34	104.29	0.71	16.46
	2000 ms	-0.34	107.34	0.65	16.05
subject 2	75 ms	-0.18	100.17	0.52	8.22
	500 ms	-0.20	102.02	0.47	8.98
	1000 ms	-0.28	103.18	0.68	12.41
	2000 ms	**0.06**	97.62	0.03	-2.83
subject	3 75 ms	-0.15	212.77	0.14	3.95
	500 ms	-0.29	204.80	0.31	7.83
	1000 ms	-0.30	203.35	0.33	8.28
	1800 ms	-0.49	201.81	0.48	13.58
subject 4	75 ms	-1.22	156.76	0.93	23.99
	500 ms	-1.50	166.01	0.89	28.15
	1000 ms	-1.42	169.19	0.81	25.82
	18000 ms	-1.50	168.80	0.83	27.83
subject 5	75 ms	-0.65	117.77	0.81	17.65
	500 ms	-0.74	119.53	0.79	20.10
	1000 ms	-0.66	115.09	0.70	18.55
	2000 ms	-0.61	121.44	0.70	16.42

Table 6.7: Result of the IMNF for dynamic contraction.

	W size	Slope	In. fr.	R-Sq	Re.Ch(%)
subject 1	75 ms	-0.15	66.71	0.49	11.72
	500 ms	-0.34	72.07	0.68	23.92
	1000 ms	-0.30	72.69	0.62	20.92
	2000 ms	-0.26	74.55	0.51	17.79
subject 2	75 ms	-0.09	66.10	0.34	6.14
	500 ms	-0.09	67.18	0.23	6.67
	1000 ms	-0.16	67.63	0.46	10.81
	2000 ms	**0.19**	62.38	0.33	-13.29
subject 3	75 ms	-0.15	189.20	0.08	4.29
	500 ms	-0.36	175.33	0.30	11.50
	1000 ms	-0.44	176.08	0.45	14.02
	1800 ms	-0.46	168.48	0.39	15.43
subject 4	75 ms	-1.33	132.67	0.92	31.20
	500 ms	-1.60	142.90	0.85	34.98
	1000 ms	-1.49	144.33	0.78	32.14
	1800 ms	-1.74	150.27	0.84	36.13
subject 5	75 ms	-0.65	87.38	0.79	24.12
	500 ms	-0.75	89.91	0.70	26.89
	1000 ms	-0.59	86.08	0.63	22.21
	2000 ms	-0.50	89.38	0.42	18.11

Table 6.8: Result of the IMDF for dynamic contraction.

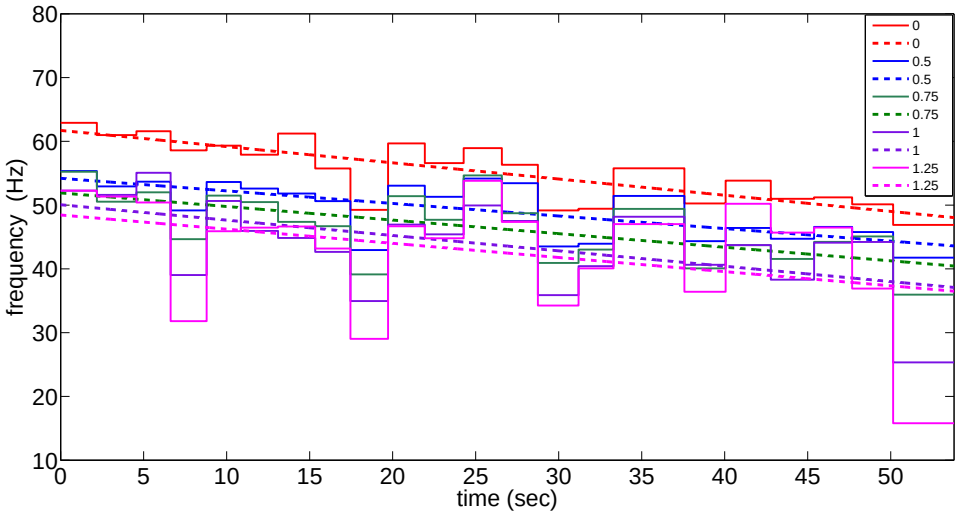

Figure 6.11: Modified WAIF for dynamic contraction for different coefficients with linear regression lines for subject 1

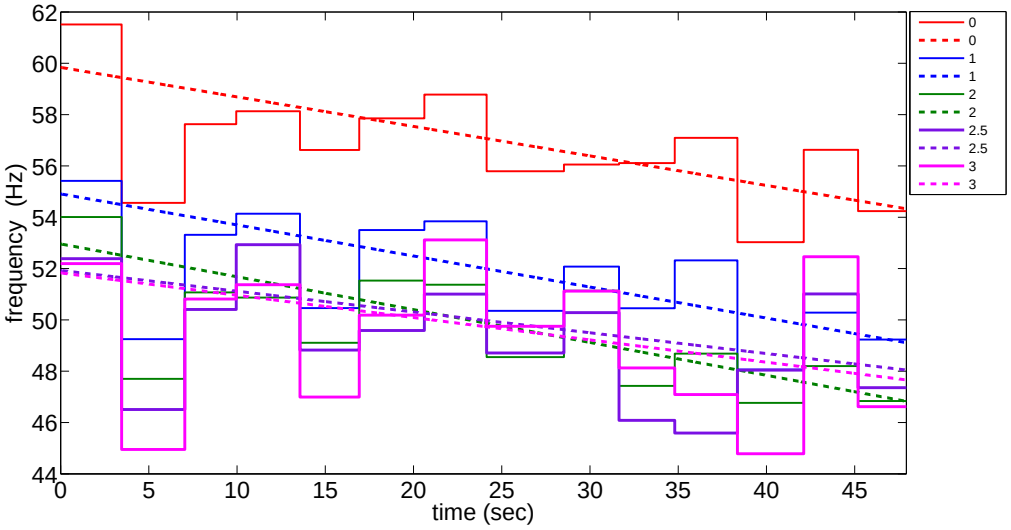

Figure 6.12: Modified WAIF for dynamic contraction for different coefficients with linear regression lines for subject 2

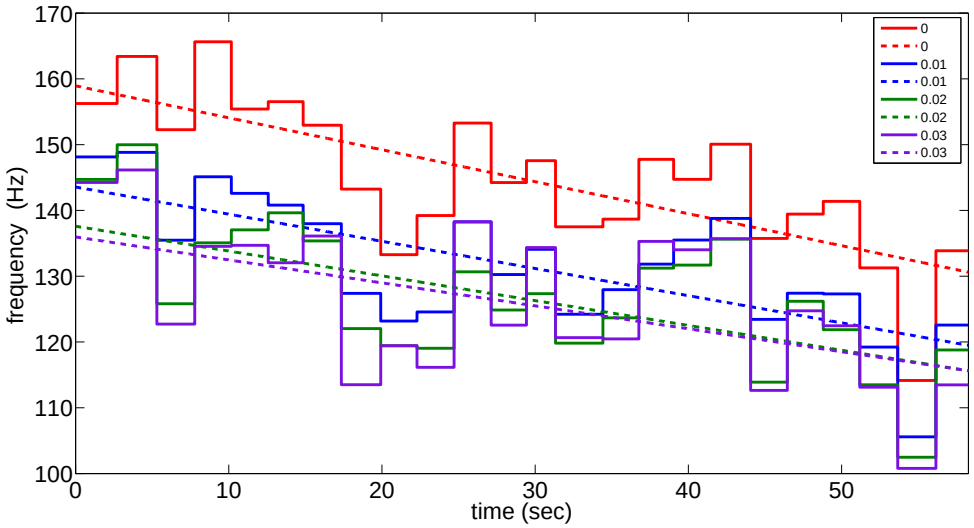

Figure 6.13: Modified WAIF for dynamic contraction for different coefficients with linear regression lines for subject 3

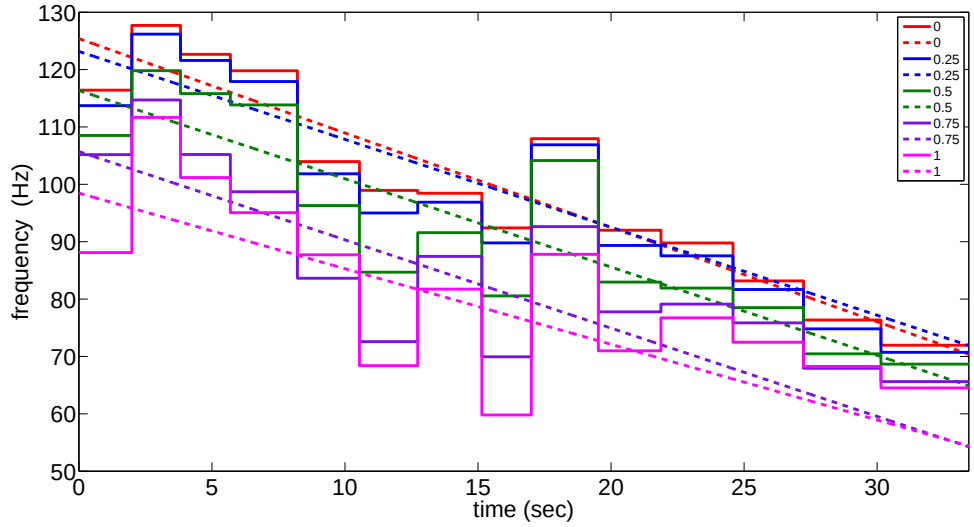

Figure 6.14: Modified WAIF for dynamic contraction for different coefficients with linear regression lines for subject 4

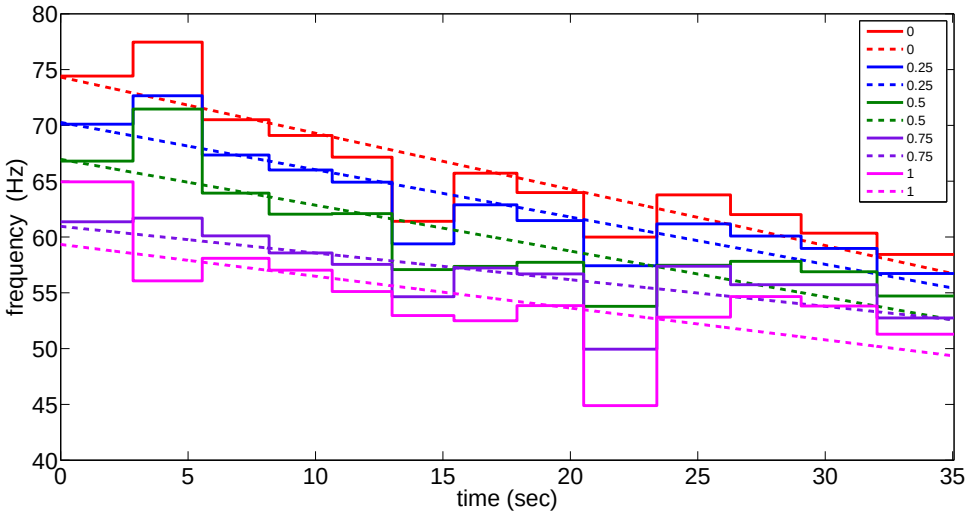

Figure 6.15: Modified WAIF for dynamic contraction for different coefficients with linear regression lines for subject 5

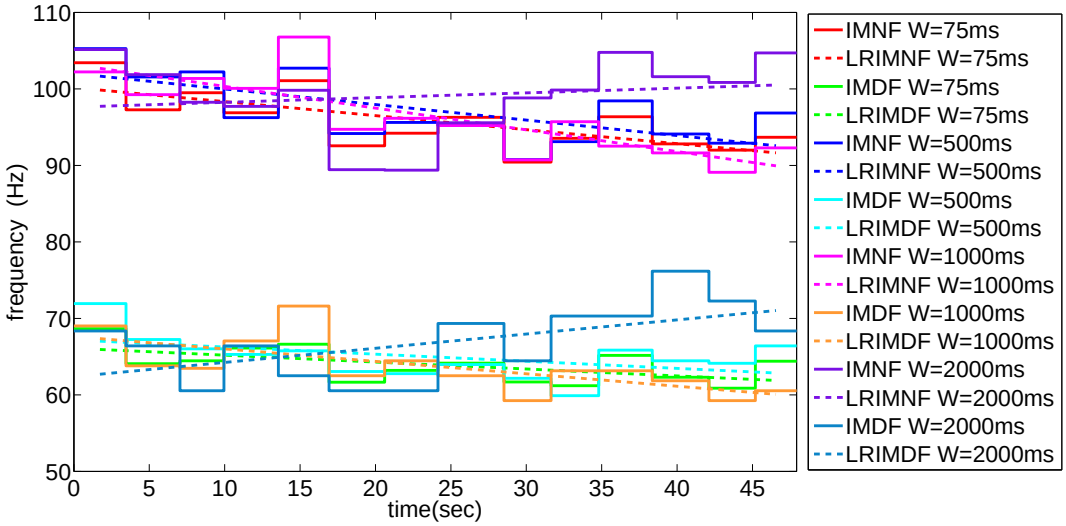

Figure 6.16: IMNF and IMDF for different windows with linear regression lines for subject 2 for dynamic contraction

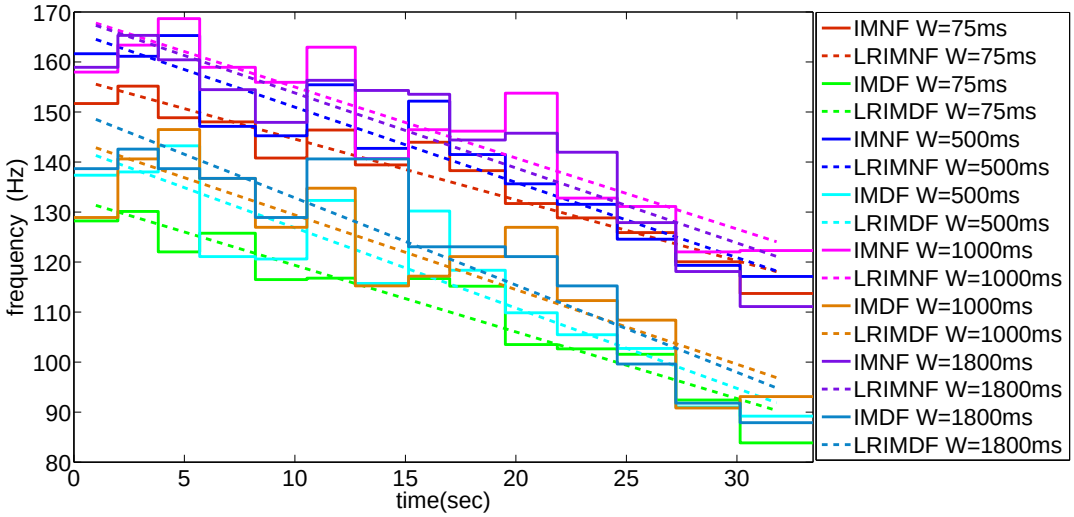

Figure 6.17: IMNF and IMDF for different windows with linear regression lines for subject 4 for dynamic contraction

6.4 Discussion

For all subjects, the MPD using a threshold that corresponded to 5% of maximum energy showed a result that extracted most of the orignal sEMG signals generated during isometric contraction. Figure 6.1 shows the original signal compared to the signal extracted by MPD for subjects 1 and 2. They are very similar. A comparison of the MPD and the spectrogram shows the advantages of the MPD since changing the window of the spectrogram result in a differnt representation of the same signal. The MPD-TFR for isometric contraction and dynamic contraction in Figure 6.2 and 6.8 shows the complexity of sEMG signals and their localized frequency, with respect to time. The spectrogram in Figure 6.3 for isometric and Figure 6.9 and 6.10 for dynamic contractions shows the strong dependence of the result on the window sizes. When the window size increases, the time localization is lost due to the uncertainty principle. Specially, MPD-TFR analysis of contraction signal data displays localized frequency characteristics as a function of time with more information than the spectrogram. Several thresholds for calculating modified WAIF during isometric exercise were investigated, using 4 different thresholds for

subject 1 and subject 2 and 2 different thresholds for the rest of the subjects. As the threshold values increased, the number of data points decreases. At a high threshold value, the number of data points was not sufficient to calculated the modified WAIF in beginning of the experiment. For dynamic contraction, the modified WAIF was calculated for each cycle so number of data points was evenly distributed even though the threshold decreases. The last point of the modified WAIF during isometric contraction showed a large drop in frequency for subject 1 as fatigue increased rapidly. This phenomena was also observed for the last cycle of modified WAIF during dynamic contraction where the average frequency dropped dramatically in subject 1 and subject 3. This correlates well to the fatigue experienced by the subject. This trend was not observed from the IMNF and IMDF result. The IMNF and IMDF that were obtained by spectrogram during isometric and dynamic contractions show that the range of the frequency for IMNF was higher than for IMDF. IMNF and IMDF with 75 ms window length for isometric contraction were very noisy. For isometric contraction, IMNF and IMDF with different window sizes displayed approximately the same slope for all, so relative change of IMFN and IMDF for isometric contraction is reported as one value as shown in the table. IMDF for isometric contraction with largest window size obtained positive slope. IMDF and IMNF for dynamic contraction with largest window size shows positive slope. Isometric and dynamic contractions of IMDF shows positive slope at largest window size. The interpretation of the data is strongly dependent on the window size that is chosen, making the results unreliable. This shows the window size effect that it has been addressed by other researchers. The relative change of modified WAIF for isometric contraction shows different values with threshold but, for dynamic contraction shows consistent change with different threshold. The relative change between IMNF and IMDF and modified WAIF for isometric contraction shows the relative change of modified WAIF was higher than the relative change of IMNF and IMDF. The relative change

between IMNF and IMDF and modified WAIF for dynamic contraction shows the relative change of modified WAIF is higher than the relative change of IMNF and IMDF except for subject 5.

Chapter 7

CONCLUSIONS AND FUTURE WORK

7.1 Conclusion

The analysis of sEMG signals with MPD gives results that are consistent with previously reported results using other analysis techniques that demonstrated lower frequency spectral content from sEMG signals as muscles fatigue occurs. The results from spectrograms both during isometric and dynamic contractions shows a shift of frequency spectral content to lower bands except for long window sizes. The trends for modified WAIF obtained by MPD and the IMNF and IMDF obtained by spectrogram were similar. The average of the relative change for both isometric and dynamic contractions from modified WAIF is higher than the relative change from IMNF and IMDF. This result could be related to resolution problem with the spectrogram method. This study shows that MPD can be used to analyze both isometric and dynamic contractions. This study demonstrated that MPD can precisely extract information from the raw sEMG signal in frequency and time. The reliability of MPD over the spectrogram method is demonstrated as it is free from the windowing effects seen in the spectrogram. It showed high potential of MPD for application for diagnostics in clinical settings where a robust method is required.

7.2 Recommendation for Future Work

In this study, localized muscle fatigue in biceps brachii was investigated to determine if the MPD technique works in this application. A sample size of five subjects was used. The high potential of MPD technique in this application was demonstrated in this study. The next steps will be to expand the study to more samples with different voluntary muscle levels to establish a dictionary for MPD. Selecting the correct dictionary for the MPD could reduce the computation requirements. Quantitative investigation of the characteristics of muscle fatigue with MPD can be used to detect fatigue in clinical applications.

[1] J. Basmajian and C. J. De Luca, *Muscle Alive*, 1st ed. Baltimore: Williams & Wilkins, 1985.

[2] M. Cifrek, V. Medved, S. Tonkovic, and S.Ostojic, "Surface EMG based muscle fatigue evaluation in biomechanics," *Clinical Biomechanics (Bristol, Avon)*, vol. 24, pp. 327–340, 2009.

[3] R. Merletti, M. Knaflitz, and C. J. De Luca, "Electrically evoked myoelectric signals," *Critical Review in Biomedical Engineering*, vol. 19, pp. 293–340, 1992.

[4] J. Basmajian and C. J. De Luca, *Electromyography - Physiology, Engineering and Noninvasive Applications*, 1st ed. Hoboken, New Jersey: John Wiley & Sons, Inc., 2004.

[5] S. Cobb and A. Forbes, "Electromyographic studies of muscular fatigue in man," *American Journal of Physiology-Legacy Content*, vol. 65, no. 2, pp. 234–251, 1923.

[6] V. Medved, "Computer algorithm for an EMG-based muscular fatigue assessment method," in *New Methods in Applied Ergonomics (International Occupational Ergonomic Symposium Proceedings)*, E. N. C. J. R. Wilson and I. Manenica, Eds. Taylor and Francis Press, 1987, p. 71.

[7] P. Bonato, S. H. Roy, M. Knaflitz, and C. J. De Luca, "Time-frequency parameters of the surface myoelectric signal for assessing muscle fatigue during cyclic dynamic contraction," *IEEE Transaction on Biomedical Engineering*, vol. 48, no. 7, pp. 745–753, July 2001.

[8] M. B. I. Reaz, M. S. Hussain, and F. Mohd-Yasin, "Techniques of EMG signal analysis: detection, processing, classification and applications," *Biological Procedures Online*, vol. 8, no. 1, pp. 11–35, 2006.

[9] J. S. Karlsson, B. Gerdle, and M. Akay, "Analyzing surface myoelectric signals recorded during isokinetic contractions," *IEEE Engineering in Medicine and Biology Magazine*, vol. 20, no. 6, pp. 97–105, Nov.-Dec. 2001.

[10] P. Bonato, G. Gagliati, and M. Knaflitz, "Analysis of myoelectric signals recorded during dynamic contractions," *IEEE Engineering in Medicine and Biology Magazine*, vol. 15, no. 6, pp. 102–111, Nov.-Dec. 1996.

[11] P. Bonato, M. S. S. Heng, J. Gonzalez-Cueto, A. Leardini, J. O'Connor, and S. H. Roy, "EMG-based measures of fatigue during a repetitive squat exercise,"

IEEE Engineering in Medicine and Biology Magazine, vol. 20, no. 6, pp. 133–143, 2001.

[12] P. Bonato and M. Knaflitz, "Time-frequency methods applied to muscle fatigue assessment during dynamic contractions," *Journal of Electromyography and Kinesiology*, vol. 9, pp. 337–350, 1999.

[13] S. Krishnan, "A new approach for estimation of instantaneous mean frequency of a time-varying signal," *EURASIP Journal of Applied Signal Processing 2005*, pp. 2848–2855, 2005.

[14] D. Chakraborty, N. Kovvali, J. Wei, A. Papandreou-Suppappola, D. Cochran, and A. Chattopadhyay, "Damage classification structural health monitoring in bolted structures using time-frequency techniques," *Journal of Intelligent Material Systems and Structures*, vol. 20, pp. 1289–1305, July 2009.

[15] S. Mallat and Z. Zhang, "Matching pursuits with time-frequency dictionaries," *IEEE Transactions on Signal processing*, vol. 41, no. 12, pp. 3397–3415, 1993.

[16] D. U. Silverthorn, *Human Physiology: an Integrated Approach*, 4th ed. San Francisco: Pearson Education, 2004.

[17] C. J. De Luca, "The use of surface electromyography in biomechanics," *Journal Applied Biomechanics*, vol. 13, pp. 135–163, 1997.

[18] E. A. Clancy, E. L. Morin, and R. Merletti, "Sampling noise-reduction and amplitude estimation issues in surface electromyography," *Journal of Electromyography and Kinesiology*, vol. 12, no. 1, pp. 1–16, 2002.

[19] K. Masuda, T. Masuda, a. M. I. T. Sadoyama, and S. Katsuta, "Changes in surface EMG parameters during static and dynamic fatiguing contractions," *Journal of Electromyography and Kinesiology*, vol. 9, no. 1, pp. 39–46, 1999.

[20] L. Brody, M. Pollock, S. Roy, C.J. De Luca, and B. Celli, "ph-induced effects on median frequency and conduction velocity of the myoelectric signal," *Journal of Applied Physiology*, vol. 71, pp. 1878–1885, 1991.

[21] E. Kwatny, D. H. Thomas, and B. Kemp, "An application of signal processing techniques to the study of myoelectric signals," *IEEE Transaction on Biomedical Engineering*, vol. 17, no. 4, pp. 303–313, 1970.

[22] F. B. Stulen and C. J. De Luca, "Frequency parameters of the myoelectric signal as measure of muscle conduction-velocity," *IEEE Transaction on Biomedical Engineering*, vol. 7, pp. 515–523, 1981.

[23] A. Georgakis, L. K. Stergioulas, and G. Giakas, "Fatigue analysis of the surface EMG signal in isometric constant force contractions using the averaged instantaneous frequency," *IEEE Transactions on Biomedical Engineering*, vol. 50, no. 2, pp. 262–265, 2003.

[24] D. Farina and R. Merletti, "Comparison of algorithms for estimation of EMG variables during voluntary isometric contraction," *Journal of Electromyography and Kinesiology*, vol. 10, pp. 337–349, 2000.

[25] M. Cifrek, S. Tonkovic, and V. Medved, "Measurement and analysis of surface myoelectric signals during fatigued cyclic dynamic contraction," *Measurement*, vol. 27, pp. 85–92, 2000.

[26] H. Xie and Z. Wang, "Mean frequency derived via Hilbert-Huang transform with application to fatigue EMG signal analysis," *Computer Methods and Programs in Biomedicine*, vol. 82, no. 2, pp. 114–120, 2006.

[27] Z. G. Zhang, H. T. Liu, S. Chan, K. D. K. Luk, and Y. Hu, "Time-dependent power spectral density estimation of surface electromyography during isometric muscle contraction: methods and comparisons," *Journal of Electromyography and Kinesiology*, vol. 20, no. 1, pp. 89–101, 2010.

[28] P. Bonato, T. D'Alessio, and M. Knaflitz, "A statistical method for the measurement of muscle activation intervals from surface myoelectric signal during gait," *IEEE Transactions on Biomedical Engineering*, vol. 45, no. 3, pp. 287–299, 1998.

[29] D. Moshou, I. Hostens, G. Papaioannou, and H. Ramon, "Dynamic muscle fatigue detection using self-organizing map," *Applied Soft Computing*, vol. 5, no. 4, pp. 391–398, 2005.

[30] P. Coorevits, L. Danneels, D. Cambier, H. Ramon, H. Druyts, K. Stefan, G. De Moor, and G. Vanderstraeten, "Correlation between short-time Fourier and continuous wavelet transforms in the analysis of localized back and hip muscle fatigue during isometric contractions," *Journal of Electromyography and Kinesiology*, vol. 18, no. 4, pp. 637–644, 2008.

[31] J. R. Potvin and L. R. Bent, "A validation of techniques using surface EMG signals from dynamic contractions to quantify muscle fatigue during repetitive

tasks," *Journal of Electromyography and Kinesiology*, vol. 7, no. 2, pp. 131–139, 1997.

[32] D. MacIsaac, P. A. Parker, and R. N. Scott, "The short time Fourier transform and muscle fatigue assessment in dynamic contractions," *Journal of Electromyography and Kinesiology*, vol. 11, no. 6, pp. 439–449, 2001.

[33] F. Hlawatsch and G. F. Boudreaux-Bartels, "Linear and quadratic time-frequency signal representations," *IEEE Signal Processing Magazine*, vol. 9, no. 2, pp. 21–67, 1992.

[34] M. R. Davies and S. S. Reisman, "Time-frequency analysis of the electromyogram during fatigue," in *Proceedings of the 20th Annual Northeast Bioengineering Conference*, 1994, pp. 93–95.

[35] L. Cohen, *Time Frequency Analysis: Theory and Application*. Englewood Cliffs, New Jersey: Prentice Hall, 1995.

[36] E. D. Ryan, J. T. Cramer, A. D. Egan, M. J. Hartman, and T. J. Herda, "Time and frequency domain responses of the mechanomyogram and electromyogram during isometric ramp contractions: A comparison of the short-time Fourier and continuous wavelet transforms," *Journal of Electromyography and Kinesiology*, vol. 18, no. 1, pp. 54–67, 2008.

[37] J. S. Karlsson, J. Yu, and M. Akay, "Time-frequency analysis of myoelectric signals during dynamic contractions: A comparative study," *IEEE Transaction on Biomedical Engineering*, vol. 47, no. 2, pp. 228–238, 2000.

[38] A. Subasi and M. K. Kiymik, "Muscle fatigue detection in EMG using time-frequency methods, ICA and neural networks," *Journal of medical systems*, vol. 34, pp. 777–785.

[39] V. Srhoj-Egekher, M. Cifrek, and V. Medved, "The application of Hilbert-Huang transform in the analysis of muscle fatigue during cyclic dynamic contractions," *Medical and Biological Engineering and Computing*, vol. 49, no. 6, pp. 659–669, 2011.

[40] P. J. Loughlin and K. L. Davidson, "Modified Cohen-Lee time-frequency distributions and instantaneous bandwidth of multicomponent," *IEEE Transactions on Signal Processing*, vol. 49, no. 6, pp. 1153–1165, 2001.

[41] G. Jones and B. Boashash, "Instantaneous frequency, instantaneous bandwidth and the analysis of multicomponent signals," in *International Conference on Acoustics, Speech and Signal Processing, 1990., Pages=2467-2470,.*

[42] S. Ghofrani, D. C. McLeronon, and A. Ayatollahi, "Estimation of instantaneous frequency and instantaneous bandwidth via adaptive signal decomposition," in *IEEE International Conference on Acoustics, Speech and Signal Processing, Proceedings.*, vol. 3, 2006, pp. III–III.

[43] L. J. Hargrove, A. M. Simon, R. D. Lipschutz, S. B. Finucane, and T. A. Kuiken, "Real-time myoelectric control of knee and ankle motions for transfemoral amputees," *The Journal of the American Medical Association*, vol. 305, no. 15, pp. 1542–1544, 2011.